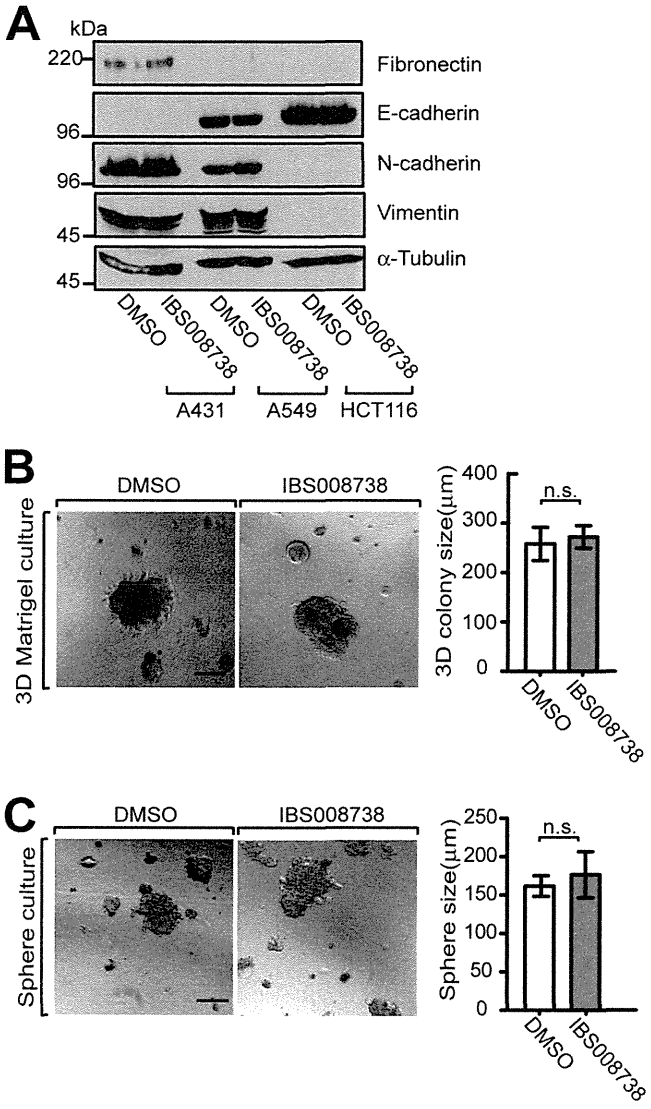

FIG 10 Effect of IBS008738 on cancer cells. (A) Human epidermal cancer A431, lung cancer A549, and colon cancer HCT116 cells were treated with IBS008738. Cell lysates were immunoblotted with the antibodies indicated. (B and C) A431 cells were cultured under sphere-forming conditions (B) or in 3D Matrigel (C). The maximum diameters of 30 cell aggregates with diameters of >150 μm were measured. IBS008738 did not enhance tumor sphere formation or the growth of A431 cells in 3D Matrigel. Bar, 200 μm. In panels B and C, the data are means and standard errors of the means. n.s., not significant.

unphosphorylated TAZ level. These changes also support the idea that IBS008738 indeed works on TAZ. Phosphate affinity SDS-PAGE analysis suggests that IBS008738 induces modifications of TAZ other than phosphorylation at serine 89. It will be intriguing and necessary to determine the molecular modifications by mass spectrometry. Phosphate affinity SDS-PAGE has additionally revealed that almost 50% of the TAZ in C2C12 cells is phosphorylated but that most of the TAZ is localized in the nucleus. This finding implies that the phosphorylated TAZ in C2C12 cells cannot be captured in the cytoplasm or is retained by the nucleus. This might be due to the limited amount of 14-3-3 or the abundance of nuclear transcriptional factors such as MyoD that interact with TAZ. The effects of IBS008738 on gene transcription are different in MCF10A and C2C12 cells. IBS008738 increases CTGF mRNA in MCF10A cells but not in C2C12 cells (Fig. 3). Likewise, IBS008738 enhances TEAD-responsive reporter activity in HEK293 cells but not in C2C12 cells. These discrepancies may reflect the different expression of TEAD and MyoD in these cells, and TAZ may select the interacting partners in a cell context-dependent manner. On the basis of our reporter and ChIP assays, we speculate that in C2C12 cells, MyoD is the main partner of TAZ under differentiation conditions and that consequently MyoD-mediated cellular outputs are most prominent in IBS008738-treated C2C12 cells.

IBS008738 enhances MyoD expression in C2C12 cells under growth conditions and accelerates myogenesis under differentiation conditions (Fig. 2). The *in vitro* interaction experiment and the immunofluorescence assay support the idea that IBS008738 augments the association of TAZ with MyoD (Fig. 4). IBS008738 stabilizes TAZ and increases its protein expression (Fig. 5). IBS008738 promotes the association of MyoD with the myogenin promoter (Fig. 3C). The binding of Pax3 to the Myf5 promoter decreased in IBS008738-treated cells. This finding is understandable, because Myf5 is known to be downregulated early in differentiation (53). As the ChIP assay was performed 24 h after differentiation, we speculated that this decrease may mirror the rapid myogenesis that occurs during IBS008738 treatment. The competition of IBS008738 with myostatin is equivocal. As SMAD2 and -3 mediate myostatin signaling and TAZ cooperates with SMAD2 and -3 in human embryonic stem cells and mouse embryos, TAZ activators are postulated to enhance myostatin signaling but IBS008738 competes with myostatin in the myogenesis of C2C12 cells (Fig. 7). We here infer again that the effect of IBS008738 on MyoD is more prominent because MyoD is more abundant than SMAD2 and -3 in C2C12 cells.

IBS008738 increases the numbers of Pax7-positive cells in the early phase and centrally nucleated fibers in injured muscles. Later, the number of Pax7-positive cells decreases while that of MyoD-positive cells increases (Fig. 8). Pax7 is thought to play dual roles in the regeneration of skeletal muscles (57). Pax7 promotes progenitors to commit to the skeletal muscle lineage but blocks terminal differentiation. Heterogeneity of satellite cells has also been discussed (58). Ten percent of quiescent satellite stem cells are $Pax7^+$ $Myf5^-$, whereas 90% of committed quiescent satellite cells are $Pax7^+$ $Myf5^+$ and are activated to subsequently coexpress MyoD, undergo limited proliferation, and then differentiate into $Pax7^-$ $MyoD^+$ cells (58, 59). We could not identify which Pax7-positive cells IBS008738 increased in the early phase after injury. We speculate the IBS008738 promotes both self-renewal of satellite stem cells and the commitment to $Pax7^+$ $Myf5^+$ satellite cells in response to injury and that it also promotes myogenic differentiation to $Pax7^+$ $Myf5^+$ $MyoD^+$ cells, which further differentiate to $Pax7^-$ $MyoD^+$ cells and at the same time harbor the subpopulation that returns to quiescent satellite cells. Thus, IBS008738 overall facilitates muscle repair with the replenishment of satellite cells. However, in order to understand how IBS008738 works, a more detailed analysis of the role of TAZ in satellite cells is necessary. IBS008738 also prevents dexamethasone-induced muscle atrophy. IBS008738 suppresses the expression of MuRF-1 and atrogin-1 and increases protein synthesis (Fig. 9). On the other hand, IBS008738 does not significantly induce EMT in the cancer cells tested (Fig. 10). These observations imply that IBS008738 may be useful for the treatment and prevention of muscle atrophy.

In this paper, we have introduced a novel cell-based assay to screen for TAZ activators. As compounds with various targets and a wide spectrum of cellular phenotypes are obtained with this assay, the collection works as a minilibrary of TAZ activators. Researchers can perform further selection based on the different cellular outputs as readouts and obtain compounds that function according to their interests.

ACKNOWLEDGMENTS

We are grateful for Hiroshi Asahara (Tokyo Medical and Dental University), Yasutomi Kamei (Kyoto Prefectural University), Hiroki Kurihara (The University of Tokyo), Yoshihiro Ogawa (Tokyo Medical and Dental University), Hiroshi Sasaki (Kumamoto University), Kenji Miyazawa (Yamanashi University), Kohei Miyazono (The University of Tokyo), Hiroshi Takayanagi (The University of Tokyo), and Sumiko Watanabe (The University of Tokyo) for materials and advice.

This work was supported by research grants from the Ministry of Education, Sports, Science, and Technology (17081008), the Japan Society for the Promotion of Science (22790275 and 22590267), the Suzuken Memorial Foundation, the Nakatomi Foundation, the Uehara Memorial Foundation, and the Naito Foundation. Z.Y. was supported by a Japanese Government (Monbukagakusho) (MEXT) scholarship.

REFERENCES

1. **Kanai F, Marignani PA, Sarbassova D, Yagi R, Hall RA, Donowitz M, Hisaminato A, Fujiwara T, Ito Y, Cantley LC, Yaffe MB.** 2000. TAZ: a novel transcriptional co-activator regulated by interactions with 14-3-3 and PDZ domain proteins. EMBO J. **19**:6778–6791. http://dx.doi.org/10.1093/emboj/19.24.6778.
2. **Hong W, Guan KL.** 2012. The YAP and TAZ transcription co-activators: key downstream effectors of the mammalian Hippo pathway. Semin. Cell Dev. Biol. **23**:785–793. http://dx.doi.org/10.1016/j.semcdb.2012.05.004.
3. **Wang K, Degerny C, Xu M, Yang XJ.** 2009. YAP, TAZ, and Yorkie: a conserved family of signal-responsive transcriptional coregulators in animal development and human disease. Biochem. Cell Biol. **87**:77–91. http://dx.doi.org/10.1139/O08-114.
4. **Sudol M.** 1994. Yes-associated protein (YAP65) is a proline-rich phosphoprotein that binds to the SH3 domain of the Yes proto-oncogene product. Oncogene **9**:2145–2152.
5. **Bao Y, Hata Y, Ikeda M, Withanage K.** 2011. Mammalian Hippo pathway: from development to cancer and beyond. J. Biochem. **149**:361–379. http://dx.doi.org/10.1093/jb/mvr021.
6. **Pan D.** 2010. The Hippo signaling pathway in development and cancer. Dev. Cell **19**:491–505. http://dx.doi.org/10.1016/j.devcel.2010.09.011.
7. **Oka T, Remue E, Meerschaert K, Vanloo B, Boucherie C, Gfeller D, Bader GD, Sidhu SS, Vandekerckhove J, Gettemans J, Sudol M.** 2010. Functional complexes between YAP2 and ZO-2 are PDZ domain-dependent, and regulate YAP2 nuclear localization and signalling. Biochem. J. **432**:461–472. http://dx.doi.org/10.1042/BJ20100870.
8. **Remue E, Meerschaert K, Oka T, Boucherie C, Vandekerckhove J, Sudol M, Gettemans J.** 2010. TAZ interacts with zonula occludens-1 and -2 proteins in a PDZ-1 dependent manner. FEBS Lett. **584**:4175–4180. http://dx.doi.org/10.1016/j.febslet.2010.09.020.
9. **Chan SW, Lim CJ, Chong YF, Pobbati AV, Huang C, Hong W.** 2011. Hippo pathway-independent restriction of TAZ and YAP by angiomotin. J. Biol. Chem. **286**:7018–7026. http://dx.doi.org/10.1074/jbc.C110.212621.
10. **Zhao B, Li L, Lu Q, Wang LH, Liu CY, Lei Q, Guan KL.** 2011. Angiomotin is a novel Hippo pathway component that inhibits YAP oncoprotein. Genes Dev. **25**:51–63. http://dx.doi.org/10.1101/gad.2000111.
11. **Dupont S, Morsut L, Aragona M, Enzo E, Giulitti S, Cordenonsi M, Zanconato F, Le Digabel J, Forcato M, Bicciato S, Elvassore N, Piccolo S.** 2011. Role of YAP/TAZ in mechanotransduction. Nature **474**:179–183. http://dx.doi.org/10.1038/nature10137.
12. **Halder G, Dupont S, Piccolo S.** 2012. Transduction of mechanical and cytoskeletal cues by YAP and TAZ. Nat. Rev. Mol. Cell Biol. **13**:591–600. http://dx.doi.org/10.1038/nrm3416.
13. **Wrighton KH.** 2011. Mechanotransduction: YAP and TAZ feel the force. Nat. Rev. Mol. Cell Biol. **12**:404. http://dx.doi.org/10.1038/nrm3145, http://dx.doi.org/10.1038/nrm3136.
14. **Azzolin L, Zanconato F, Bresolin S, Forcato M, Basso G, Bicciato S, Cordenonsi M, Piccolo S.** 2012. Role of TAZ as mediator of Wnt signaling. Cell **151**:1443–1456. http://dx.doi.org/10.1016/j.cell.2012.11.027.
15. **Imajo M, Miyatake K, Iimura A, Miyamoto A, Nishida E.** 2012. A molecular mechanism that links Hippo signalling to the inhibition of Wnt/β-catenin signalling. EMBO J. **31**:1109–1122. http://dx.doi.org/10.1038/emboj.2011.487.
16. **Varelas X, Miller BW, Sopko R, Song S, Gregorieff A, Fellouse FA, Sakuma R, Pawson T, Hunziker W, McNeill H, Wrana JL, Attisano L.** 2010. The Hippo pathway regulates Wnt/beta-catenin signaling. Dev. Cell **18**:579–591. http://dx.doi.org/10.1016/j.devcel.2010.03.007.
17. **de Cristofaro T, Di Palma T, Ferraro A, Corrado A, Lucci V, Franco R, Fusco A, Zannini M.** 2011. TAZ/WWTR1 is overexpressed in papillary thyroid carcinoma. Eur. J. Cancer **47**:926–933. http://dx.doi.org/10.1016/j.ejca.2010.11.008.
18. **Wang L, Shi S, Guo Z, Zhang X, Han S, Yang A, Wen W, Zhu Q.** 2013. Overexpression of YAP and TAZ is an independent predictor of prognosis in colorectal cancer and related to the proliferation and metastasis of colon cancer cells. PLoS One **8**:e65539. http://dx.doi.org/10.1371/journal.pone.0065539.
19. **Wei Z, Wang Y, Li Z, Yuan C, Zhang W, Wang D, Ye J, Jiang H, Wu Y, Cheng J.** 29 March 2013. Overexpression of Hippo pathway effector TAZ in tongue squamous cell carcinoma: correlation with clinicopathological features and patients' prognosis. J. Oral Pathol. Med. (Epub ahead of print.) http://dx.doi.org/10.1111/jop.12062.
20. **Yuen HF, McCrudden CM, Huang YH, Tham JM, Zhang X, Zeng Q, Zhang SD, Hong W.** 2013. TAZ expression as a prognostic indicator in colorectal cancer. PLoS One **8**:e54211. http://dx.doi.org/10.1371/journal.pone.0054211.
21. **Zhou Z, Hao Y, Liu N, Raptis L, Tsao MS, Yang X.** 2011. TAZ is a novel oncogene in non-small cell lung cancer. Oncogene **30**:2181–2186. http://dx.doi.org/10.1038/onc.2010.606.
22. **Bhat KP, Salazar KL, Balasubramaniyan V, Wani K, Heathcock L, Hollingsworth F, James JD, Gumin J, Diefes KL, Kim SH, Turski A, Azodi Y, Yang Y, Doucette T, Colman H, Sulman EP, Lang FF, Rao G, Copray S, Vaillant BD, Aldape KD.** 2011. The transcriptional coactivator TAZ regulates mesenchymal differentiation in malignant glioma. Genes Dev. **25**:2594–2609. http://dx.doi.org/10.1101/gad.176800.111.
23. **Chan SW, Lim CJ, Guo K, Ng CP, Lee I, Hunziker W, Zeng Q, Hong W.** 2008. A role for TAZ in migration, invasion, and tumorigenesis of breast cancer cells. Cancer Res. **68**:2592–2598. http://dx.doi.org/10.1158/0008-5472.CAN-07-2696.
24. **Cordenonsi M, Zanconato F, Azzolin L, Forcato M, Rosato A, Frasson C, Inui M, Montagner M, Parenti AR, Poletti A, Daidone MG, Dupont S, Basso G, Bicciato S, Piccolo S.** 2011. The Hippo transducer TAZ confers cancer stem cell-related traits on breast cancer cells. Cell **147**:759–772. http://dx.doi.org/10.1016/j.cell.2011.09.048.
25. **Hao J, Zhang Y, Jing D, Li Y, Li J, Zhao Z.** 2014. Role of Hippo signaling in cancer stem cells. J. Cell Physiol. **229**:266–270. http://dx.doi.org/10.1002/jcp.24455.
26. **Skinner M.** 2012. Cancer stem cells: TAZ takes centre stage. Nat. Rev. Cancer **12**:82–83. http://dx.doi.org/10.1038/nrc3210.
27. **Chan SW, Lim CJ, Huang C, Chong YF, Gunaratne HJ, Hogue KA, Blackstock WP, Harvey KF, Hong W.** 2011. WW domain-mediated interaction with Wbp2 is important for the oncogenic property of TAZ. Oncogene **30**:600–610. http://dx.doi.org/10.1038/onc.2010.438.
28. **Chan SW, Lim CJ, Loo LS, Chong YF, Huang C, Hong W.** 2009. TEADs mediate nuclear retention of TAZ to promote oncogenic transformation. J. Biol. Chem. **284**:14347–14358. http://dx.doi.org/10.1074/jbc.M901568200.
29. **Zhang H, Liu CY, Zha ZY, Zhao B, Yao J, Zhao S, Xiong Y, Lei QY, Guan KL.** 2009. TEAD transcription factors mediate the function of TAZ in cell growth and epithelial-mesenchymal transition. J. Biol. Chem. **284**:13355–13362. http://dx.doi.org/10.1074/jbc.M900843200.
30. **Park KS, Whitsett JA, Di Palma T, Hong JH, Yaffe MB, Zannini M.** 2004. TAZ interacts with TTF-1 and regulates expression of surfactant protein-C. J. Biol. Chem. **279**:17384–17390. http://dx.doi.org/10.1074/jbc.M312569200.
31. **Murakami M, Nakagawa M, Olson EN, Nakagawa O.** 2005. A WW domain protein TAZ is a critical coactivator for TBX5, a transcription factor implicated in Holt-Oram syndrome. Proc. Natl. Acad. Sci. U. S. A. **102**:18034–18039. http://dx.doi.org/10.1073/pnas.0509109102.
32. **Varelas X, Sakuma R, Samavarchi-Tehrani P, Peerani R, Rao BM,**

Dembowy J, Yaffe MB, Zandstra PW, Wrana JL. 2008. TAZ controls Smad nucleocytoplasmic shuttling and regulates human embryonic stem-cell self-renewal. Nat. Cell Biol. **10**:837–848. http://dx.doi.org/10.1038/ncb1748.

33. **Varelas X, Samavarchi-Tehrani P, Narimatsu M, Weiss A, Cockburn K, Larsen BG, Rossant J, Wrana JL.** 2010. The Crumbs complex couples cell density sensing to Hippo-dependent control of the TGF-β-SMAD pathway. Dev. Cell **19**:831–844. http://dx.doi.org/10.1016/j.devcel.2010.11.012.
34. **Hong JH, Hwang ES, McManus MT, Amsterdam A, Tian Y, Kalmukova R, Mueller E, Benjamin T, Spiegelman BM, Sharp PA, Hopkins N, Yaffe MB.** 2005. TAZ, a transcriptional modulator of mesenchymal stem cell differentiation. Science **309**:1074–1078. http://dx.doi.org/10.1126/science.1110955.
35. **Cui CB, Cooper LF, Yang X, Karsenty G, Aukhil I.** 2003. Transcriptional coactivation of bone-specific transcription factor Cbfa1 by TAZ. Mol. Cell. Biol. **23**:1004–1013. http://dx.doi.org/10.1128/MCB.23.3.1004-1013.2003.
36. **Jeong H, Bae S, An SY, Byun MR, Hwang JH, Yaffe MB, Hong JH, Hwang ES.** 2010. TAZ as a novel enhancer of MyoD-mediated myogenic differentiation. FASEB J. **24**:3310–3320. http://dx.doi.org/10.1096/fj.09-151324.
37. **Murakami M, Tominaga J, Makita R, Uchijima Y, Kurihara Y, Nakagawa O, Asano T, Kurihara H.** 2006. Transcriptional activity of Pax3 is co-activated by TAZ. Biochem. Biophys. Res. Commun. **339**:533–539. http://dx.doi.org/10.1016/j.bbrc.2005.10.214.
38. **Benhaddou A, Keime C, Ye T, Morlon A, Michel I, Jost B, Mengus G, Davidson I.** 2012. Transcription factor TEAD4 regulates expression of myogenin and the unfolded protein response genes during C2C12 cell differentiation. Cell Death Differ. **19**:220–231. http://dx.doi.org/10.1038/cdd.2011.87.
39. **Zhu X, Topouzis S, Liang LF, Stotish RL.** 2004. Myostatin signaling through Smad2, Smad3 and Smad4 is regulated by the inhibitory Smad7 by a negative feedback mechanism. Cytokine **26**:262–272. http://dx.doi.org/10.1016/j.cyto.2004.03.007.
40. **Judson RN, Gray SR, Walker C, Carroll AM, Itzstein C, Lionikas A, Zammit PS, De Bari C, Wackerhage H.** 2013. Constitutive expression of Yes-associated protein (Yap) in adult skeletal muscle fibres induces muscle atrophy and myopathy. PLoS One **8**:e59622. http://dx.doi.org/10.1371/journal.pone.0059622.
41. **Watt KI, Judson R, Medlow P, Reid K, Kurth TB, Burniston JG, Ratkevicius A, De Bari C, Wackerhage H.** 2010. Yap is a novel regulator of C2C12 myogenesis. Biochem. Biophys. Res. Commun. **393**:619–624. http://dx.doi.org/10.1016/j.bbrc.2010.02.034.
42. **Sayer AA, Robinson SM, Patel HP, Shavlakadze T, Cooper C, Grounds MD.** 2013. New horizons in the pathogenesis, diagnosis and management of sarcopenia. Age Ageing **42**:145–150. http://dx.doi.org/10.1093/ageing/afs191.
43. **Bao Y, Nakagawa K, Yang Z, Ikeda M, Withanage K, Ishigami-Yuasa M, Okuno Y, Hata S, Nishina H, Hata Y.** 2011. A cell-based assay to screen stimulators of the Hippo pathway reveals the inhibitory effect of dobutamine on the YAP-dependent gene transcription. J. Biochem. **150**:199–208. http://dx.doi.org/10.1093/jb/mvr063.
44. **Ikeda M, Kawata A, Nishikawa M, Tateishi Y, Yamaguchi M, Nakagawa K, Hirabayashi S, Bao Y, Hidaka S, Hirata Y, Hata Y.** 2009. Hippo pathway-dependent and -independent roles of RASSF6. Sci. Signal. **2**:ra59. http://dx.doi.org/10.1126/scisignal.2000300.
45. **Hirabayashi S, Nakagawa K, Sumita K, Hidaka S, Kawai T, Ikeda M, Kawata A, Ohno K, Hata Y.** 2008. Threonine 74 of MOB1 is a putative key phosphorylation site by MST2 to form the scaffold to activate nuclear Dbf2-related kinase 1. Oncogene **27**:4281–4292. http://dx.doi.org/10.1038/onc.2008.66.
46. **Bao Y, Sumita K, Kudo T, Withanage K, Nakagawa K, Ikeda M, Ohno K, Wang Y, Hata Y.** 2009. Roles of mammalian sterile 20-like kinase 2-dependent phosphorylations of Mps one binder 1B in the activation of nuclear Dbf2-related kinases. Genes Cells **14**:1369–1381. http://dx.doi.org/10.1111/j.1365-2443.2009.01354.x.
47. **Ota M, Sasaki H.** 2008. Mammalian Tead proteins regulate cell proliferation and contact inhibition as transcriptional mediators of Hippo signaling. Development **135**:4059–4069. http://dx.doi.org/10.1242/dev.027151.
48. **Kobayashi N, Goto K, Horiguchi K, Nagata M, Kawata M, Miyazawa K, Saitoh M, Miyazono K.** 2007. c-Ski activates MyoD in the nucleus of myoblastic cells through suppression of histone deacetylases. Genes Cells **12**:375–385. http://dx.doi.org/10.1111/j.1365-2443.2007.01052.x.
49. **Nelson JD, Denisenko O, Bomsztyk K.** 2006. Protocol for the fast chromatin immunoprecipitation (ChIP) method. Nat. Protoc. **1**:179–185. http://dx.doi.org/10.1038/nprot.2006.27.
50. **Goodman CA, Mabrey DM, Frey JW, Miu MH, Schmidt EK, Pierre P, Hornberger TA.** 2011. Novel insights into the regulation of skeletal muscle protein synthesis as revealed by a new nonradioactive in vivo technique. FASEB J. **25**:1028–1039. http://dx.doi.org/10.1096/fj.10-168799.
51. **Ikeda M, Hirabayashi S, Fujiwara N, Mori H, Kawata A, Iida J, Bao Y, Sato Y, Iida T, Sugimura H, Hata Y.** 2007. Ras-association domain family protein 6 induces apoptosis via both caspase-dependent and caspase-independent pathways. Exp. Cell Res. **313**:1484–1495. http://dx.doi.org/10.1016/j.yexcr.2007.02.013.
52. **Hong JH, Yaffe MB.** 2006. TAZ: a beta-catenin-like molecule that regulates mesenchymal stem cell differentiation. Cell Cycle **5**:176–179. http://dx.doi.org/10.4161/cc.5.2.2362.
53. **Lindon C, Montarras D, Pinset C.** 1998. Cell cycle-regulated expression of the muscle determination factor Myf5 in proliferating myoblasts. J. Cell Biol. **140**:111–118. http://dx.doi.org/10.1083/jcb.140.1.111.
54. **Schakman O, Kalista S, Barbé C, Loumaye A, Thissen JP.** 2013. Glucocorticoid-induced skeletal muscle atrophy. Int. J. Biochem. Cell Biol. **45**:2163–2172. http://dx.doi.org/10.1016/j.biocel.2013.05.036.
55. **Byun MR, Jeong H, Bae SJ, Kim AR, Hwang ES, Hong JH.** 2012. TAZ is required for the osteogenic and anti-adipogenic activities of kaempferol. Bone **50**:364–372. http://dx.doi.org/10.1016/j.bone.2011.10.035.
56. **Jang EJ, Jeong H, Kang JO, Kim NJ, Kim MS, Choi SH, Yoo SE, Hong JH, Bae MA, Hwang ES.** 2012. TM-25659 enhances osteogenic differentiation and suppresses adipogenic differentiation by modulating the transcriptional co-activator TAZ. Br. J. Pharmacol. **165**:1584–1594. http://dx.doi.org/10.1111/j.1476-5381.2011.01664.x.
57. **Olguín HC, Pisconti A.** 2012. Marking the tempo for myogenesis: Pax7 and the regulation of muscle stem cell fate decisions. J. Cell. Mol. Med. **16**:1013–1025. http://dx.doi.org/10.1111/j.1582-4934.2011.01348.x.
58. **Wang YX, Rudnicki MA.** 2012. Satellite cells, the engines of muscle repair. Nat. Rev. Mol. Cell Biol. **13**:127–133. http://dx.doi.org/10.1038/nrm3265.
59. **Zammit PS, Golding JP, Nagata Y, Hudon V, Partridge TA, Beauchamp JR.** 2004. Muscle satellite cells adopt divergent fates: a mechanism for self-renewal? J. Cell Biol. **166**:347–357. http://dx.doi.org/10.1083/jcb.200312007.

Biochemical and Biophysical Research Communications 443 (2014) 917–923

Contents lists available at ScienceDirect

Biochemical and Biophysical Research Communications

journal homepage: www.elsevier.com/locate/ybbrc

The PDZ-binding motif of Yes-associated protein is required for its co-activation of TEAD-mediated *CTGF* transcription and oncogenic cell transforming activity

Tadanori Shimomura, Norio Miyamura, Shoji Hata, Ryota Miura, Jun Hirayama *, Hiroshi Nishina *

Department of Developmental and Regenerative Biology, Medical Research Institute, Tokyo Medical and Dental University, 1-5-45 Yushima, Bunkyo-ku, Tokyo 113-8510, Japan

ARTICLE INFO

Article history:
Received 11 December 2013
Available online 28 December 2013

Keywords:
YAP
Hippo pathway
CTGF
TEAD

ABSTRACT

YAP is a transcriptional co-activator that acts downstream of the Hippo signaling pathway and regulates multiple cellular processes, including proliferation. Hippo pathway-dependent phosphorylation of YAP negatively regulates its function. Conversely, attenuation of Hippo-mediated phosphorylation of YAP increases its ability to stimulate proliferation and eventually induces oncogenic transformation. The C-terminus of YAP contains a highly conserved PDZ-binding motif that regulates YAP's functions in multiple ways. However, to date, the importance of the PDZ-binding motif to the oncogenic cell transforming activity of YAP has not been determined. In this study, we disrupted the PDZ-binding motif in the YAP (5SA) protein, in which the sites normally targeted by Hippo pathway-dependent phosphorylation are mutated. We found that loss of the PDZ-binding motif significantly inhibited the oncogenic transformation of cultured cells induced by YAP (5SA). In addition, the increased nuclear localization of YAP (5SA) and its enhanced activation of TEAD-dependent transcription of the cell proliferation gene *CTGF* were strongly reduced when the PDZ-binding motif was deleted. Similarly, in mouse liver, deletion of the PDZ-binding motif suppressed nuclear localization of YAP (5SA) and YAP (5SA)-induced *CTGF* expression. Taken together, our results indicate that the PDZ-binding motif of YAP is critical for YAP-mediated oncogenesis, and that this effect is mediated by YAP's co-activation of TEAD-mediated *CTGF* transcription.

1. Introduction

The Yes-associated protein (YAP) is a transcriptional co-activator that regulates multiple cellular processes by activating several transcription factors [1]. Recently, YAP was shown to play an important role in organ size control and to be inhibited by the Hippo signaling pathway [2–4]. In mouse liver, either transgenic overexpression of YAP or knock-out of Hippo pathway genes causes enlargement of this organ and the eventual development of hepatic tumors [5,6]. In cultured cells, YAP overexpression promotes proliferation and induces oncogenic transformation by activating TEAD-mediated transcription of the cell proliferation gene connective tissue growth factor (*CTGF*) [7,8]. Thus, the proper control of YAP activity is critical for maintaining tissue homeostasis in animals.

YAP functions are regulated by multiple post-translational modifications, including phosphorylation, SUMOylation, acetylation, and methylation [9–13]. Among these, phosphorylation is the best characterized regulatory event. For example, cell–cell contact triggers the Hippo pathway to phosphorylate YAP and thereby inactivate it, inhibiting cell proliferation. This phosphorylation is mediated by Lats kinases, which are essential components of the Hippo pathway. Lats-mediated phosphorylation of serine 127 (Ser-127) of human YAP (hYAP) promotes its recognition and cytoplasmic retention by 14-3-3 protein [9], while phosphorylation of hYAP Ser-381 induces hYAP ubiquitination and degradation [10]. Thus, the Hippo pathway negatively regulates the transcriptional co-activation capacity of YAP by inducing its cytoplasmic localization and protein degradation.

YAP contains a highly conserved PDZ-binding motif in its C-terminal domain, and this motif reportedly contributes to the regulation of YAP's functions. For example, Oka et al. showed that the interaction of the tight junction protein zonula occludens 2 (ZO2) with YAP's PDZ-binding motif facilitates nuclear localization of YAP [14]. In another study, it was reported that YAP stabilizes p73 to promote apoptosis, and that YAP's PDZ-binding motif is required for this proapoptotic function [15]. Although these studies

Abbreviations: YAP, Yes-associated protein; CTGF, connective tissue growth factor; TEAD, TEA domain family member; TAZ, transcriptional co-activator with PDZ-binding motif.

* Corresponding authors. Fax: +81 3 5803 5829.
E-mail addresses: hirayama.dbio@mri.tmd.ac.jp (J. Hirayama), nishina.dbio@mri.tmd.ac.jp (H. Nishina).

0006-291X/$ - see front matter © 2013 Elsevier Inc. All rights reserved.
http://dx.doi.org/10.1016/j.bbrc.2013.12.100

demonstrate that the PDZ-binding motif is important for regulating YAP's normal functions, the role of this motif in controlling the oncogenic cell transforming activity of YAP has not been characterized.

In this study, we investigated whether the PDZ-binding motif of hYAP is involved in its ability to transform cultured cells using the hYAP (5SA) mutant, which is not under the negative control of the Hippo pathway due to mutation of key phosphorylation sites [9]. As a result, hYAP (5SA) is constitutively activated and abnormally increased in a cell's nucleus. YAP co-transcriptional activity is thus elevated, inducing the oncogenic transformation of cultured cells. We found that disruption of the PDZ-binding motif strongly inhibited these properties of hYAP (5SA) both in cultured cells and mouse liver. Our results thus provide several lines of evidence indicating that the PDZ-binding motif is involved in regulating the nuclear localization of YAP and its co-activator function. In particular, we show that loss of this motif reduces TEAD-mediated transcription of *CTGF*, damping down YAP's oncogenic transforming activity.

2. Materials and methods

2.1. Plasmids

The mouse *CTGF* gene promoter was amplified by PCR and cloned into the pGL3-Basic vector (Promega). The *CTGF* promoter region spans codons −708 to −220 (+1 is the start codon) and contains the TEAD-binding element. Mutations were introduced into Myc-hYAP/pCS2 using PCR-based site-directed mutagenesis to generate mutant forms of hYAP described in each Figure. To inactivate the PDZ-binding motif, the *hYap* cDNA sequences corresponding to the last five amino acids of the hYAP protein were deleted. Other plasmids used in this study have been described elsewhere [12].

2.2. Cells, transfection, and luciferase assay

293T and NIH3T3 cells were grown in Dulbecco's modified Eagle's medium (Invitrogen) supplemented with 10% fetal bovine serum. For luciferase reporter assays, 293T cells were transfected with 40 ng firefly luciferase reporter plasmid, 20 ng sea pansy luciferase reporter plasmid [pRL-SV40 (Promega)], and the appropriate expression plasmids (indicated in each Figure) using Fugene HD (Promega). At 24 h post-transfection, cell lysates were prepared and dual luciferase assays performed using the dual-luciferase reporter assay system (Promega). Firefly and sea pansy luciferase activities were quantified by means of a luminometer, with the firefly luciferase activity normalized for transfection efficiency based on the sea pansy luciferase activity.

2.3. Antibodies

Anti-Myc, anti-lamin A/C, and anti-actin antibodies were purchased from Santa Cruz; rat anti-HA antibody from Roche Diagnostics Corp.; rabbit anti-HA antibody from Immunology Consultants Laboratory; and anti-β-tubulin antibody from Cell Signaling Technology.

2.4. Co-immunoprecipitation

Co-immunoprecipitation was performed as previously described [16], with some modifications. 293T cells were transfected with the expression plasmids described in each Figure. Transfected cells were washed with phosphate-buffered saline, homogenized in binding buffer (150 mM NaCl, 1 mM EDTA, 0.5% Nonidet P-40, 5% glycerol and 20 mM Tris–HCl, pH 7.4) containing protease inhibitor, and clarified by centrifugation. Total protein from the supernatant was incubated at 4 °C with rabbit anti-HA antibody and 20 μl protein G-Sepharose beads. The beads were washed four times with binding buffer, boiled in SDS sample buffer. The supernatant was fractionated by SDS–PAGE and analyzed by Western blotting as described below.

2.5. Western blotting

Immunoprecipitated materials and total cell extracts obtained as described above were fractionated by SDS–PAGE and transferred electrophoretically onto polyvinylidene difluoride membranes. Membranes were blocked with Blocking One (Nacalai Tesque) or 2% skim milk and incubated for 10 h at 4 °C with the antibodies indicated in each Figure. The blots were then incubated with the appropriate secondary antibodies plus peroxidase-conjugated anti-mouse, anti-rabbit, anti-rat, or anti-goat IgG antibodies (Santa Cruz) and developed with the ECL Western blotting detection system (Amersham Biosciences).

2.6. Immunofluorescence

Frozen sections of mouse liver were attached to APS-coated glass slides (Matsunami Glass). After blocking with 5% BSA in TBS, the slides were incubated with primary antibodies followed by fluorescent tag-conjugated secondary antibodies. Nuclei and plasma membranes were counterstained with Hoechst 33342 or phalloidin (both from Invitrogen), respectively.

2.7. Quantitation of nuclear protein in cultured cells

Levels of YAP localized in cellular nuclei were calculated as follows. The signal intensities of bands of YAP proteins appearing on Western blots were measured using the Quantity One (Bio-Rad) and normalized to the signal intensity of the band representing the nuclear protein laminA/C (value 1). The signal intensities of total hYAPs were normalized for protein loading based on the signal intensity of the band representing actin (value 2). Value 1 was divided by value 2 to obtain the value for nuclear hYAP protein.

2.8. Mice

All mice used in this study were of the C57BL/6J genetic background. All experimental procedures in this study were approved by the Institutional Animal Care and Use Committee of Tokyo Medical and Dental University.

2.9. Plasmid injections into living mice

Manipulated genes were expressed in hepatocytes of living mice by the hydrodynamic tail vein injection (HTVi) system. Briefly, each gene of interest was cloned into the pLIVE vector and suspended in *Trans*IT-EE Hydrodynamic Delivery Solution (Mirus Bio). Plasmids were injected into tail veins of mice.

3. Results

3.1. Deletion of the PDZ-binding motif of hYAP (5SA) abolishes its oncogenic transforming activity

We first compared the effects of transient expression of Myc-tagged plasmids expressing wild type hYAP [hYAP (WT)] or several mutant forms of hYAP in NIH3T3 cells. NIH3T3 cells transfected with hYAP (WT) and cultured for an extended period stopped proliferating when they reached saturation density (Fig. 1A). Similar

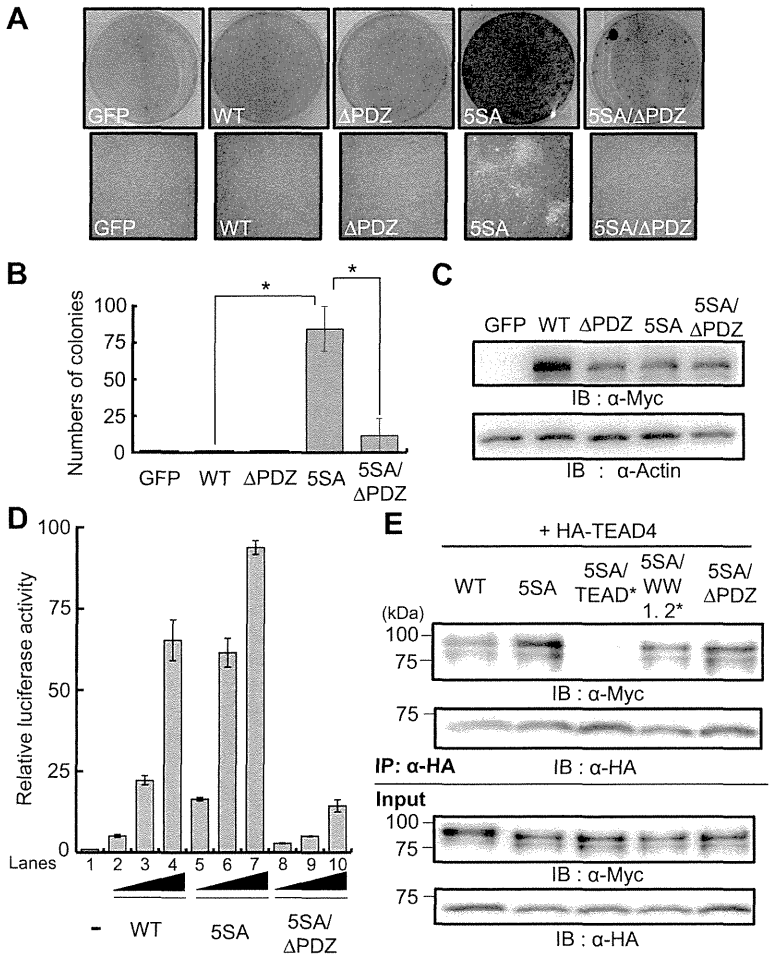

Fig. 1. The PDZ-binding motif of hYAP (5SA) is required for its oncogenic activity. (A) The cell transforming activity of wild type hYAP and various mutant forms of hYAP were determined by colony formation assays. Vectors expressing GFP (control), wild type hYAP (WT), WT hYAP lacking its PDZ-binding motif (ΔPDZ), the hYAP (5SA) mutant (5SA), or the hYAP (5SA) mutant lacking its PDZ-binding motif (5SA/ΔPDZ), were transiently expressed in NIH3T3 cells. At 18 days post-transfection, colonies were visualized by crystal violet staining (upper panels). The corresponding phase-contrast images of these NIH3T3 cells are also shown (lower panels). (B) The numbers of colonies in the plates in (A) were counted. Values are the mean ± S.E. ($n = 3$ plates/group). *$P < 0.05$. (C) Protein levels of WT hYAP and its mutant forms in the cells in (A) were confirmed by Western blot (WB). (D) Transcriptional co-activation capacities of WT hYAP and its mutant forms were determined by luciferase reporter assays. Wild type hYAP, hYAP (5SA) or hYAP (5SA/ΔPDZ) was co-expressed in 293T cells with TEAD, and transactivation of a luciferase reporter plasmid containing the mouse *CTGF* promoter was examined. Values are the mean ± S.E. ($n = 3$) of luciferase activity relative to that in the sample containing only the reporter plasmid (set to 1). The difference between the results shown in lanes 2 and 5, 3 and 6, 5 and 8, 6 and 9, or 7 and 10 is statistically significant ($P < 0.01$). The difference between the results shown in lanes 4 and 7 is statistically significant ($P < 0.05$). (E) HA-tagged TEAD was co-expressed in 293T cells with Myc-tagged WT hYAP or its mutant forms. Lysates were immunoprecipitated (IP) with anti-HA antibody and analyzed by WB with anti-Myc antibody to detect hYAP proteins, or with anti-HA antibody to detect TEAD. Input: Total cell extracts were analyzed by WB with anti-Myc to detect WT hYAP and its mutant forms, or with anti-HA antibody to detect TEAD. 5SA/TEAD*, hYAP (5SA) with a mutated TEAD-binding domain; 5SA/WW1.2*, hYAP (5SA) with mutated WW domains.

results were observed for cells expressing GFP (control), or hYAP (WT) missing its PDZ-binding motif (hYAP-ΔPDZ). However, when NIH3T3 cells were transiently transfected with the hYAP (5SA) mutant, some of these cells re-initiated proliferation after confluence was reached. Nodules were formed in which the cells began to pile up, a feature of the oncogenic transformation phenotype (Fig. 1A–C). These findings are consistent with a previous report [10] and confirm that Hippo pathway-dependent suppression of hYAP activity inhibits its ability to transform cells. Strikingly, the oncogenic transforming activity of hYAP (5SA) was significantly reduced by deletion of its PDZ-binding motif [hYAP (5SA/ΔPDZ)] (Fig. 1A and B), suggesting that this motif plays an important role in the cell transforming activity of hYAP (5SA).

Previous work has demonstrated that YAP-dependent co-activation of TEAD-mediated transcription of the cell proliferation gene *CTGF* is an important step in the oncogenic cell transformation induced by hYAP (5SA) [7]. We then used a luciferase reporter assay to test whether the PDZ-binding motif of hYAP (5SA) could drive TEAD-mediated transcription from the *CTGF* promoter. As reported elsewhere [9], co-expression of hYAP (WT) enhanced TEAD-mediated *CTGF* transcription in a dose-dependent manner (Fig. 1D). As expected, *CTGF* transcription was significantly increased above this enhanced level when hYAP (5SA) was co-expressed. In contrast, the co-transcriptional activity of co-expressed hYAP (5SA/ΔPDZ) was markedly diminished, indicating that deletion of the PDZ-binding motif impairs the ability of hYAP (5SA) to co-activate TEAD-mediated *CTGF* transcription.

One explanation for our observations could be that deletion of hYAP (5SA)'s PDZ-binding motif affected its interaction with TEAD. To test this possibility, we used co-immunoprecipitation to examine the ability of WT and mutant forms of hYAP to interact with TEAD. HA-TEAD was co-expressed in cultured cells with Myc-hYAP (WT), Myc-hYAP (5SA), Myc-hYAP (5SA/WW1. 2*), or Myc-hYAP (5SA/ΔPDZ), all of which possess an intact TEAD-binding domain.

When cell lysates were subjected to immunoprecipitation with anti-HA antibody, we found that all four forms of hYAP successfully co-immunoprecipitated with HA-TEAD (Fig. 1E). In contrast, hYAP (5SA) bearing a mutated TEAD-binding domain (5SA/TEAD*; negative control) [8] did not co-immunoprecipitate with HA-TEAD. Because hYAP (5SA/ΔPDZ) maintained its TEAD-binding ability, we concluded that the reduced co-transcriptional capacity of hYAP (5SA/ΔPDZ) is not due to an inability to interact with TEAD.

3.2. Deletion of the PDZ-binding motif induces the cytoplasmic localization of hYAP (5SA)

We next tested the effect of PDZ-binding motif deletion on the subcellular localization of hYAP (5SA). Myc-hYAP (WT), Myc-hYAP (5SA) or Myc-hYAP (5SA/ΔPDZ) was expressed in cultured cells and hYAP sub-cellular localization was determined by cell fractionation and Western blotting. hYAP (WT) was detected in both the nucleus and cytoplasm (Fig. 2). Nuclear localization of hYAP (5SA) was significantly increased compared to that of hYAP (WT). These results are consistent with previous reports showing that Hippo-mediated YAP phosphorylation is necessary for its cytoplasmic retention [5,9]. Importantly, compared to Myc-hYAP (5SA), a higher concentration of Myc-hYAP (5SA/ΔPDZ) was present in the cytoplasm than in the nucleus (Fig. 2). Thus, deletion of the PDZ-binding motif blocks the nuclear localization of hYAP (5SA), an event that would account for its impaired promotion of TEAD-mediated *CTGF* transcription.

3.3. Addition of NLS does not rescue nuclear localization of hYAP (ΔPDZ)

To examine whether the addition of a nuclear localization sequence (NLS) to hYAP (ΔPDZ) could restore its nuclear localization, we generated a series of constructs in which the SV40 NLS sequence was inserted into the N-terminus of hYAP (WT) or hYAP (ΔPDZ). The subcellular localization of each of these NLS-fused hYAP proteins was then determined after transfection into 293T cells. We found that the addition of SV40 NLS significantly increased the nuclear localization of hYAP (WT) (Fig. 3A and B), indicating that the NLS was indeed functional. However, NLS addition did not increase the nuclear localization of hYAP (ΔPDZ) (Fig. 3A and B). We also investigated whether NLS fusion altered the co-transcriptional activity of hYAPs during TEAD-mediated *CTGF* transcription. As expected, the activity of NLS-fused hYAP (WT) was significantly greater than that of hYAP (WT) (Fig. 3C). On the other hand, the addition of SV40 NLS had no effect on the already limited co-transcriptional activity of hYAP (ΔPDZ). These results indicate that NLS-dependent nuclear import is insufficient to compensate for the defect in hYAP nuclear localization imposed by loss of its PDZ-binding motif.

3.4. Deletion of the PDZ-binding motif suppresses hYAP (5SA)-mediated co-activation of CTGF transcription in mouse liver

To determine if our results in cultured cells could be extended to the tissues of living mice, we used HTVi to test the effect of

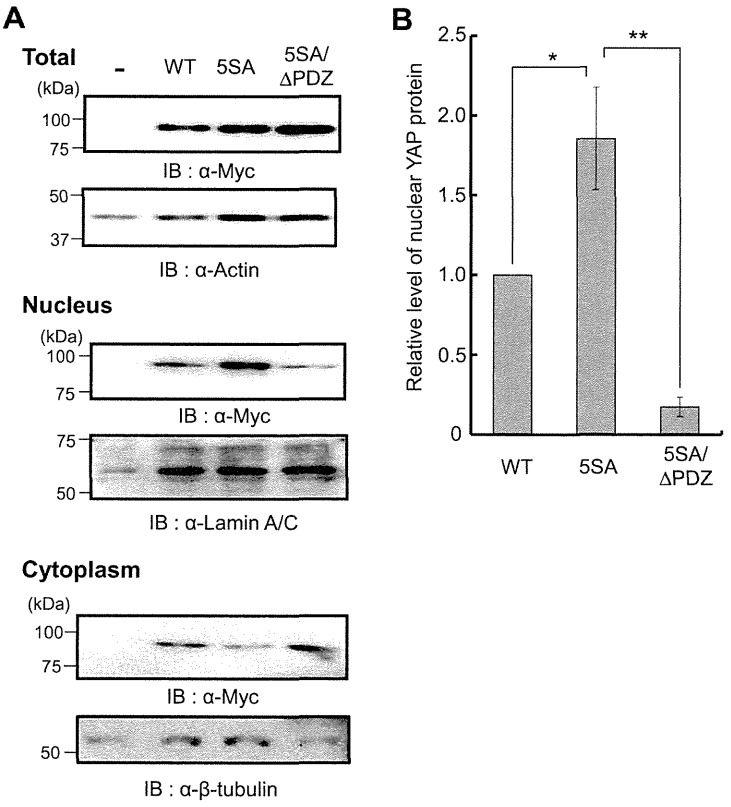

Fig. 2. The PDZ-binding motif of hYAP (5SA) is required for its nuclear localization in cultured cells. (A) Vectors expressing Myc-tagged hYAP (WT), hYAP (5SA), or hYAP (5SA/ΔPDZ) were individually transfected into 293T cells. Lysates were prepared, with some set aside (Total) and the rest subjected to subcellular fractionation to generate cytoplasmic and nuclear fractions. In each case, protein levels of Myc-tagged hYAP (WT) and the indicated mutant hYAP forms were determined by WB with anti-Myc antibody. The presence of the cytoplasmic marker β-tubulin and the nuclear marker lamin A/C in the appropriate fractions was confirmed by WB with the corresponding antibodies. Results shown are representative of three experiments. (B) Quantitative analysis of the nuclear localization of WT hYAP and its mutant forms in the cells in (A). The signal intensities in each lane of the "Nucleus" panel of (A) were measured as described in Section 2. Data are expressed relative to the value of the hYAP (WT) sample (set to 1). Values are the mean ± S.E. ($n = 3$). $^*P < 0.05$, $^*P < 0.01$.

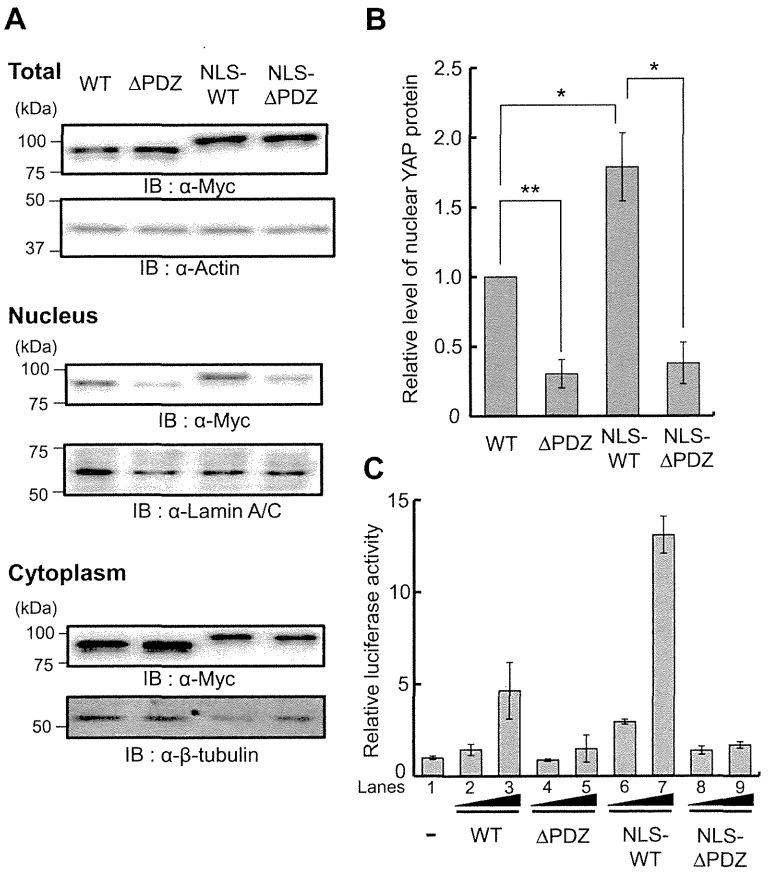

Fig. 3. The SV40 NLS has no effect on the cytoplasmic localization of hYAP (ΔPDZ). (A) Vectors expressing Myc-tagged hYAP (WT), hYAP (ΔPDZ), NLS-fused hYAP (WT), or NLS-fused YAP (ΔPDZ) were individually transfected into 293T cells and subcellular fractionation and analysis were performed as for Fig. 2A. (B) Quantitative analysis of the nuclear localization of hYAP (WT) and the indicated mutant hYAP forms was performed as for Fig. 2B. $^{*}P < 0.05$,$^{**}P < 0.01$. (C) The transcriptional co-activation capacities of hYAP (WT) and the indicated mutant forms were determined by luciferase reporter assay as for Fig. 1D. The difference between the results shown in lanes 7 and 9 is statistically significant ($P < 0.01$). The difference between the results shown in lanes 2 and 6, 3 and 7, or 6 and 8 is statistically significant ($P < 0.05$).

PDZ-binding motif deletion on YAP's subcellular localization in mouse liver. This system results in the safe and efficient delivery of naked nucleic acids to the liver of living mice. Myc-tagged plasmids expressing hYAP (WT), hYAP (5SA) or hYAP (5SA/ΔPDZ) were introduced into mouse liver by HTVi, and nuclear or cytoplasmic localization of each hYAP form was determined by immunofluorescence. When exogenously expressed in mouse liver, Myc-hYAP (WT) was almost exclusively localized in the cytoplasm (Fig. 4A and B). In contrast, Myc-hYAP (5SA) was concentrated in the nucleus and gave only a weak diffuse signal in the cytoplasm. These results confirm that, as in cultured cells, the Hippo pathway regulates YAP subcellular localization in mouse liver. Importantly, hYAP (5SA/ΔPDZ) was mainly located in the cytoplasm, replicating our earlier findings and showing that the PDZ-binding motif of hYAP is crucial for YAP nuclear localization *in vivo*.

We then examined expression levels of *CTGF* in livers of mice that had received HTVi introduction of hYAP (WT) or its mutant forms. As shown in Fig. 4C, levels of *CTGF* mRNA in mouse liver expressing exogenous hYAP (5SA) were much higher than in mouse liver expressing exogenous hYAP (WT). Once again, deletion of the PDZ-binding motif abolished the induction of *CTGF* expression by hYAP (5SA). Taken together, our results clearly demonstrate that the PDZ-binding motif of YAP is required for YAP's nuclear translocation *in vivo* and thus its ability to co-activate *CTGF* transcription.

4. Discussion

YAP can act as an oncoprotein that promotes excessive cell proliferation and induces tumorigenic transformation in both *in vitro* and *in vivo* systems [5,7,17]. It is known that the TEAD family of transcription factors plays an essential role in this YAP-induced proliferation and oncogenic transformation [8]. YAP activates TEAD-mediated transcription of *CTGF*, a cell proliferation gene, which triggers cell growth and eventually oncogenic transformation. Thus, in studies of the constitutively active YAP (5SA) mutant, disruption of either its TEAD-binding domain or transactivation domain suppresses tumorigenic cell transformation [8,9]. We have shown here that the PDZ-binding motif is also required for YAP's oncogenic cell transforming activity (Fig. 1A–C). Deletion of the PDZ-binding motif inhibited the nuclear translocation of hYAP (5SA), reducing its ability to co-activate TEAD-mediated transcription in the nucleus (Fig. 1D, Fig. 2). In addition, *CTGF* expression was significantly decreased in cells expressing hYAP (5SA/ΔPDZ) compared with cells expressing hYAP (5SA) *in vivo* (Fig. 4). Our results therefore imply that dysfunction of the PDZ-binding motif disrupts YAP/TEAD-dependent transcription of the *CTGF* gene in the nucleus, suppressing hYAP (5SA)-induced oncogenic transformation.

Previous studies have established that Hippo-mediated phosphorylation of hYAP promotes its recognition by 14-3-3 protein

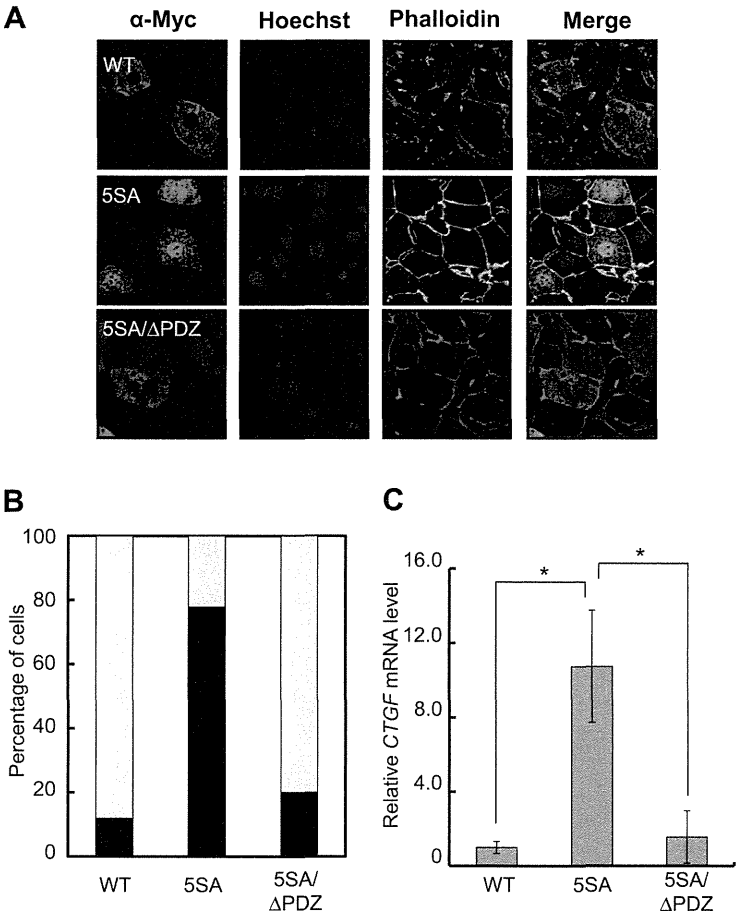

Fig. 4. The PDZ-binding motif is important for the nuclear localization and transcriptional co-activation capacity of hYAP (5SA) in mouse liver. (A) Vectors expressing Myc-tagged hYAP (WT), hYAP (5SA), or hYAP (5SA/ΔPDZ) were individually introduced into mouse liver by HTVi (see Section 2). Myc-tagged hYAPs were detected by staining with anti-Myc followed by fluorescein-conjugated secondary antibody (red). Nuclei and plasma membranes were counterstained with Hoechst 33342 (blue) or phalloidin (green), respectively. (B) Quantitative analysis of the subcellular localization of the exogenous hYAP proteins in (A). For each experimental group, 50–60 cells were evaluated to determine if the fluorescent hYAP protein was predominantly nuclear (black bars) or cytoplasmic (white bars) in localization. Data shown are the percentage of cells showing nuclear vs. cytoplasmic hYAP. (C) Extracts of livers from the mice in (A) were examined by RT-PCR analysis to detect *CTGF* mRNA levels. Data were normalized to expression of mouse *Gapdh* mRNA and are expressed relative to the value of the hYAP (WT) sample (set to 1). Results shown are the mean ± SEM ($n = 3$). $^*P < 0.05$. (For interpretation of the references to color in this figure legend, the reader is referred to the web version of this article.)

and consequently its cytoplasmic retention [9]. We found that deletion of the PDZ-binding motif induced cytoplasmic localization of hYAP (5SA) (Fig. 2 and Fig. 4), suggesting that PDZ-binding motif-dependent nuclear localization of YAP is independent of Hippo-mediated regulation. TAZ is a paralog of YAP, and deletion of the PDZ-binding motif of TAZ inhibits its nuclear localization induced by disruption of Lats-mediated phosphorylation [18]. It is possible that the same subcellular localization control mechanisms operate for both TAZ and YAP.

It has been reported both that the tight junction protein ZO2 binds to YAP's PDZ-binding motif, facilitating YAP's nuclear localization, and that the NLS of ZO2 is required for the ZO2-mediated nuclear localization of YAP [14]. Our results indicate that this NLS-mediated mechanism is insufficient for PDZ-binding motif-dependent nuclear translocation of YAP (Fig. 3). Conceivably, ZO2 binding to YAP's PDZ-binding motif mediates the interaction of YAP with the other factor(s) promoting nuclear localization, or induces a conformational change in YAP that promotes its nuclear translocation. The identification of novel proteins interacting with the PDZ-binding motif of YAP and the delineation of their roles in the control of YAP activity will lead to a clearer understanding of YAP's biological functions.

Acknowledgments

This work was supported in part by research Grants from the Ministry of Education, Culture, Sports, Science and Technology of Japan (J.H. and H.N.), and from the Ministry of Health, Labour and Welfare of Japan (H.N.).

References

[1] R. Yagi, L.F. Chen, K. Shigesada, Y. Murakami, Y. Ito, A WW domain-containing yes-associated protein (YAP) is a novel transcriptional co-activator, EMBO J. 18 (1999) 2551–2562.
[2] G. Halder, R.L. Johnson, Hippo signaling: growth control and beyond, Development 138 (2011) 9–22.
[3] A. Genevet, N. Tapon, The Hippo pathway and apico-basal cell polarity, Biochem. J. 436 (2011) 213–224.
[4] B. Zhao, K. Tumaneng, K.L. Guan, The Hippo pathway in organ size control, tissue regeneration and stem cell self-renewal, Nat. Cell Biol. 13 (2011) 877–883.
[5] J. Dong, G. Feldmann, J. Huang, S. Wu, N. Zhang, S.A. Comerford, M.F. Gayyed, R.A. Anders, A. Maitra, D. Pan, Elucidation of a universal size-control mechanism in Drosophila and mammals, Cell 130 (2007) 1120–1133.
[6] D. Zhou, C. Conrad, F. Xia, J.S. Park, B. Payer, Y. Yin, G.Y. Lauwers, W. Thasler, J.T. Lee, J. Avruch, N. Bardeesy, Mst1 and Mst2 maintain hepatocyte quiescence and suppress hepatocellular carcinoma development through inactivation of the Yap1 oncogene, Cancer Cell 16 (2009) 425–438.

[7] M. Overholtzer, J. Zhang, G.A. Smolen, B. Muir, W. Li, D.C. Sgroi, C.X. Deng, J.S. Brugge, D.A. Haber, Transforming properties of YAP, a candidate oncogene on the chromosome 11q22 amplicon, Proc. Natl. Acad. Sci. USA 103 (2006) 12405–12410.

[8] B. Zhao, X. Ye, J. Yu, L. Li, W. Li, S. Li, J.D. Lin, C.Y. Wang, A.M. Chinnaiyan, Z.C. Lai, K.L. Guan, TEAD mediates YAP-dependent gene induction and growth control, Genes Dev. 22 (2008) 1962–1971.

[9] B. Zhao, X. Wei, W. Li, R.S. Udan, Q. Yang, J. Kim, J. Xie, T. Ikenoue, J. Yu, L. Li, P. Zheng, K. Ye, A. Chinnaiyan, G. Halder, Z.C. Lai, K.L. Guan, Inactivation of YAP oncoprotein by the Hippo pathway is involved in cell contact inhibition and tissue growth control, Genes Dev. 21 (2007) 2747–2761.

[10] B. Zhao, L. Li, K. Tumaneng, C.Y. Wang, K.L. Guan, A coordinated phosphorylation by Lats and CK1 regulates YAP stability through SCF(beta-TRCP), Genes Dev. 24 (2010) 72–85.

[11] E. Lapi, S. Di Agostino, S. Donzelli, H. Gal, E. Domany, G. Rechavi, P.P. Pandolfi, D. Givol, S. Strano, X. Lu, G. Blandino, PML, YAP, and p73 are components of a proapoptotic autoregulatory feedback loop, Mol. Cell 32 (2008) 803–814.

[12] S. Hata, J. Hirayama, H. Kajiho, K. Nakagawa, Y. Hata, T. Katada, M. Furutani-Seiki, H. Nishina, A novel acetylation cycle of transcription co-activator Yes-associated protein that is downstream of Hippo pathway is triggered in response to SN2 alkylating agents, J. Biol. Chem. 287 (2012) 22089–22098.

[13] M.J. Oudhoff, S.A. Freeman, A.L. Couzens, F. Antignano, E. Kuznetsova, P.H. Min, J.P. Northrop, B. Lehnertz, D. Barsyte-Lovejoy, M. Vedadi, C.H. Arrowsmith, H. Nishina, M.R. Gold, F.M. Rossi, A.C. Gingras, C. Zaph, Control of the hippo pathway by Set7-dependent methylation of Yap, Dev. Cell 26 (2013) 188–194.

[14] T. Oka, E. Remue, K. Meerschaert, B. Vanloo, C. Boucherie, D. Gfeller, G.D. Bader, S.S. Sidhu, J. Vandekerckhove, J. Gettemans, M. Sudol, Functional complexes between YAP2 and ZO-2 are PDZ domain-dependent, and regulate YAP2 nuclear localization and signalling1, Biochem. J. 432 (2010) 461–472.

[15] T. Oka, M. Sudol, Nuclear localization and pro-apoptotic signaling of YAP2 require intact PDZ-binding motif, Genes Cells 14 (2009) 607–615.

[16] Y. Uchida, T. Osaki, T. Yamasaki, T. Shimomura, S. Hata, K. Horikawa, S. Shibata, T. Todo, J. Hirayama, H. Nishina, Involvement of stress kinase mitogen-activated protein kinase kinase 7 in regulation of mammalian circadian clock, J. Biol. Chem. 287 (2012) 8318–8326.

[17] L. Zender, M.S. Spector, W. Xue, P. Flemming, C. Cordon-Cardo, J. Silke, S.T. Fan, J.M. Luk, M. Wigler, G.J. Hannon, D. Mu, R. Lucito, S. Powers, S.W. Lowe, Identification and validation of oncogenes in liver cancer using an integrative oncogenomic approach, Cell 125 (2006) 1253–1267.

[18] F. Kanai, P.A. Marignani, D. Sarbassova, R. Yagi, R.A. Hall, M. Donowitz, A. Hisaminato, T. Fujiwara, Y. Ito, L.C. Cantley, M.B. Yaffe, TAZ: a novel transcriptional co-activator regulated by interactions with 14-3-3 and PDZ domain proteins, EMBO J. 19 (2000) 6778–6791.

OPEN ACCESS Freely available online

PLOS ONE

The Hippo Pathway Controls a Switch between Retinal Progenitor Cell Proliferation and Photoreceptor Cell Differentiation in Zebrafish

Yoichi Asaoka[1]*, Shoji Hata[1], Misako Namae[1], Makoto Furutani-Seiki[2], Hiroshi Nishina[1]*

1 Department of Developmental and Regenerative Biology, Medical Research Institute, Tokyo Medical and Dental University, Tokyo, Japan, **2** Centre for Regenerative Medicine, Department of Biology and Biochemistry, University of Bath, Claverton Down, Bath, United Kingdom

Abstract

The precise regulation of numbers and types of neurons through control of cell cycle exit and terminal differentiation is an essential aspect of neurogenesis. The Hippo signaling pathway has recently been identified as playing a crucial role in promoting cell cycle exit and terminal differentiation in multiple types of stem cells, including in retinal progenitor cells. When Hippo signaling is activated, the core Mst1/2 kinases activate the Lats1/2 kinases, which in turn phosphorylate and inhibit the transcriptional cofactor Yap. During mouse retinogenesis, overexpression of Yap prolongs progenitor cell proliferation, whereas inhibition of Yap decreases this proliferation and promotes retinal cell differentiation. However, to date, it remains unknown how the Hippo pathway affects the differentiation of distinct neuronal cell types such as photoreceptor cells. In this study, we investigated whether Hippo signaling regulates retinogenesis during early zebrafish development. Knockdown of zebrafish *mst2* induced early embryonic defects, including altered retinal pigmentation and morphogenesis. Similar abnormal retinal phenotypes were observed in zebrafish embryos injected with a constitutively active form of *yap* [*(yap (5SA)*]. Loss of Yap's TEAD-binding domain, two WW domains, or transcription activation domain attenuated the retinal abnormalities induced by *yap (5SA)*, indicating that all of these domains contribute to normal retinal development. Remarkably, *yap (5SA)*-expressing zebrafish embryos displayed decreased expression of transcription factors such as *otx5* and *crx*, which orchestrate photoreceptor cell differentiation by activating the expression of *rhodopsin* and other photoreceptor cell genes. Co-immunoprecipitation experiments revealed that Rx1 is a novel interacting partner of Yap that regulates photoreceptor cell differentiation. Our results suggest that Yap suppresses the differentiation of photoreceptor cells from retinal progenitor cells by repressing Rx1-mediated transactivation of photoreceptor cell genes during zebrafish retinogenesis.

Citation: Asaoka Y, Hata S, Namae M, Furutani-Seiki M, Nishina H (2014) The Hippo Pathway Controls a Switch between Retinal Progenitor Cell Proliferation and Photoreceptor Cell Differentiation in Zebrafish. PLoS ONE 9(5): e97365. doi:10.1371/journal.pone.0097365

Editor: Hiroyasu Nakano, Toho University School of Medicine, Japan

Received January 24, 2014; **Accepted** April 17, 2014; **Published** May 14, 2014

Funding: This work was supported by a Grant-in-Aid for Scientific Research on Innovative Areas from the Ministry of Education, Culture, Sports, Science, and Technology of Japan, a Grant-in-Aid for Scientific Research (C) from the Japan Society for the Promotion of Science, and a Grant-in-Aid from the Ministry of Health, Labor and Welfare of Japan. The funders had no role in study design, data collection and analysis, decision to publish, or preparation of the manuscript.

Competing Interests: The authors have declared that no competing interests exist.

* E-mail: y-asaoka.dbio@mri.tmd.ac.jp (YA); nishina.dbio@mri.tmd.ac.jp (HN)

Introduction

In the vertebrate embryonic nervous system, multipotent neural progenitor cells proliferate and differentiate into diverse neuronal and glial cell types that eventually build up functional neural circuits such as the retina [1,2]. The retina is a delicate multilayered neural epithelium composed of six types of neurons and one major type of glial cell [3]. During the course of retinal development, retinal progenitor cells (RPCs) either continue to proliferate or exit mitosis and differentiate into various neuronal cell types. This process is tightly regulated and ensures that the proper numbers and types of differentiated cells needed to assemble a functional retinal circuitry are produced [1,2]. A fundamental mystery in retinal development has been the identity of the molecular mechanism controlling the developmental switch between RPC self-renewal and differentiation. Although rodent models have provided valuable insights into the molecular basis of vertebrate retinal development [4], the zebrafish (*Danio rerio*) is a good alternative in which to seek the definitive answer to this question [5,6]. Fertilized zebrafish eggs rapidly develop *ex utero* into transparent embryos, facilitating retinal observations and experimental manipulations such as morpholino knockdown and the use of transgenic technology. In addition, aspects of retinal morphogenesis and histology, as well as the molecular components governing retinal development, are highly conserved between zebrafish and mammals.

The FGF, Shh, Wnt and Notch signaling pathways have all been identified as affecting retinal cell proliferation and differentiation [7]. For instance, the Notch pathway normally suppresses photoreceptor cell production in the mammalian retina, whereas inhibition of Notch signaling enhances the expression of the *Otx2* and *Crx* genes, which encode transcription factors (TFs) expressed exclusively in photoreceptor cells [8–10]. Another important pathway recently shown to be involved in regulating the balance between RPC maintenance and differentiation is the Hippo signaling cascade [11]. Hippo signaling plays fundamental roles in organ size control, stem cell maintenance, and progenitor differentiation in a variety of tissues, including the central nervous

system (CNS) [12–14]. When activated by a developmental cue, the Hippo core Mst1/2 kinases activate the Lats1/2 kinases, which in turn phosphorylate and negatively regulate the transcriptional cofactor Yap. Control of Yap in this way modulates the transcription of many genes required for tissue-specific cell differentiation [15].

The importance of the Hippo pathway in retinogenesis has been revealed by studies in mice and zebrafish. For example, gene knockout mice lacking Sav1, a component of the Hippo pathway, showed impaired organization of the retinal epithelium during neurogenesis [16]. In a different study, forced expression of Yap in the developing mouse retina led to RPC proliferation and inhibition of retinal differentiation [11]. In zebrafish, knockdown of Yap decreased progenitor cell populations in the CNS, including in the eye [17]. These observations suggest that the Hippo pathway is essential for controlling the balance of self-renewal and differentiation in developing RPCs. However, the precise molecular mechanism by which the Hippo pathway regulates the differentiation of specific types of retinal neurons has remained obscure. In particular, there is little information on the target retinal TF(s) activated downstream of the Hippo-Yap pathway. In this study, we show that the TF Rx1, a novel interacting partner of Yap, is a missing piece of this puzzle and contributes to retinal photoreceptor cell differentiation regulated by the Hippo-Yap pathway. We propose a model in which Yap regulates the timing of photoreceptor cell differentiation by suppressing Rx1-mediated transactivation of the *otx*, *crx* and *rhodopsin* genes.

Results

Mst2 is Required for Early Embryogenesis in Zebrafish

To unravel the role of Hippo signaling in early zebrafish development, we first examined whether zebrafish *mst* functions during early embryogenesis. We performed BLAST searches with human *MST1* and *MST2* genes to predict the sequence of zebrafish *mst* cDNA and found that the zebrafish has only one *mst2* ortholog. The predicted amino acid sequence of the protein encoded by the zebrafish *mst2* gene is approximately 90% identical to the sequences of the human and mouse Mst2 proteins, and contains the evolutionarily conserved autophosphorylation site and SARAH domain that are important for Mst activation (Fig. S1A). A phylogenetic analysis confirmed that the zebrafish *mst2* gene was clustered with those of several vertebrate species, including teleosts (Fig. S1B). To determine the functionality of the zebrafish *mst2* gene, we performed a morpholino (MO)-mediated loss-of-function analysis. Zebrafish embryos treated with *mst2* MO (*mst2* morphants) showed a range of abnormal phenotypes at 52 hours post-fertilization (hpf), from short body length (SL) to abnormal eye pigmentation (AP) and abnormal eye morphology (AM) (Fig. 1A and 1B). RT-PCR analysis confirmed that microinjection of *mst2* MO had effectively prevented correct splicing of the targeted pre-mRNA (Fig. S1C and S1D). These results demonstrate that Mst2 plays a critical role in early zebrafish embryogenesis.

Yap Activity has Important Effects on Early Zebrafish Development

Since Yap is a key effector molecule downstream of the Hippo signaling pathway [12,13], we determined whether overexpression of *yap* induced morphological phenotypes similar to those observed in *mst2* morphants. The amino acid sequence of the Yap protein in the small fish medaka is 85% identical to that of the zebrafish Yap protein and contains the five sites normally phosphorylated by Lats in vertebrate Yap (Fig. S2A). It is now well established that the Hippo pathway regulates Yap's phosphorylation, subcellular localization, and transcriptional coactivator activity, and that this control mechanism is evolutionarily conserved among vertebrates [18]. Some post-translational modifications of Yap, such as its acetylation, are also highly conserved among vertebrates [19]. These observations gave us confidence that medaka Yap (WT) would be functionally comparable with zebrafish Yap (WT) in our experiments. In addition, we generated a constitutively active form of medaka Yap called Yap (5SA) in which the five sites normally targeted by Hippo pathway-dependent phosphorylation were mutated to alanine [20]. Normal zebrafish embryos that were injected with *in vitro*-transcribed medaka *yap (WT)* mRNA were indistinguishable from *EGFP* mRNA-injected control embryos during the first 2 days of development (Fig. 2A). However, by 48 hpf, embryos that had been injected with constitutively active *yap (5SA)* mRNA exhibited the same range of abnormal phenotypes (SL, AP and AM) as seen in the *mst2* morphants (Fig. 2B). These observations indicate that Yap acts downstream of Mst2 to influence early zebrafish development.

The TEAD-binding, WW and Transcription Activation Domains of Yap are Required for Normal Zebrafish Embryogenesis

To define which functional domains of Yap are important for early zebrafish development, we created a series of *yap (5SA)* constructs bearing mutations or deletions inactivating specific Yap domains (Fig. 3). Injection of *yap (5SA)* mRNA led to the same range of developmental defects as presented in Fig. 2B (SL, 19%; AP+SL, 15%; AM+AP+SL, 42%; normal phenotype, 4%; N = 26). Similar results were observed for embryos injected with *yap (5SA)* mRNA missing its SH3-binding domain [*yap (5SA/ΔSH3)*]. In contrast, expression of a *yap (5SA)* mRNA with a defect in the TEAD-binding domain [*yap (5SA/TEAD*)*] reduced the frequency of abnormal phenotypes (AP+SL, 11%; normal phenotype, 68%; N = 19). In addition, the majority of embryos injected with *yap (5SA)* mRNA mutated in both the WW1 and WW2 domains [*yap (5SA/WW1*, 2*)*] exhibited a normal phenotype (AM+AP+SL, 5%; normal phenotype, 89%; N = 19). Finally, almost all embryos injected with *yap (5SA)* mRNA missing its transcription activation domain [*yap (5SA/ΔTA)*] showed a normal phenotype (AM+AP+SL, 3%; normal phenotype, 97%; N = 31). Taken together, these observations demonstrate that overexpression of the TEAD-binding, WW and transcription activation domains of Yap can alter early zebrafish development, and that these domains are therefore critical for normal zebrafish morphogenesis.

Yap Activity Plays a Direct Role in Zebrafish Retinogenesis

Our experiments in Figure 3 showed that injection of *yap (5SA)* mRNA caused abnormal retinal development and body axis malformation. However, it was not clear whether the retinal abnormality was a primary consequence of Yap hyperactivation or a secondary effect caused by the failure in body axis formation. To distinguish between these possibilities, we examined in detail the timing of the emergence of the SL phenotype in *yap (5SA)* mRNA-injected zebrafish embryos. Overexpression of *yap (5SA)* mRNA induced no obvious defects during gastrulation or anterior-posterior axis formation (Fig. S2B), consistent with previous work [21]. After gastrulation, however, the SL phenotype became apparent at 18–21 hpf (Fig. S2C), indicating that increased Yap activity affects the elongation of the body axis during the segmentation period. To minimize the effects of body axis malformation, we generated a *yap (5SA)* construct under the

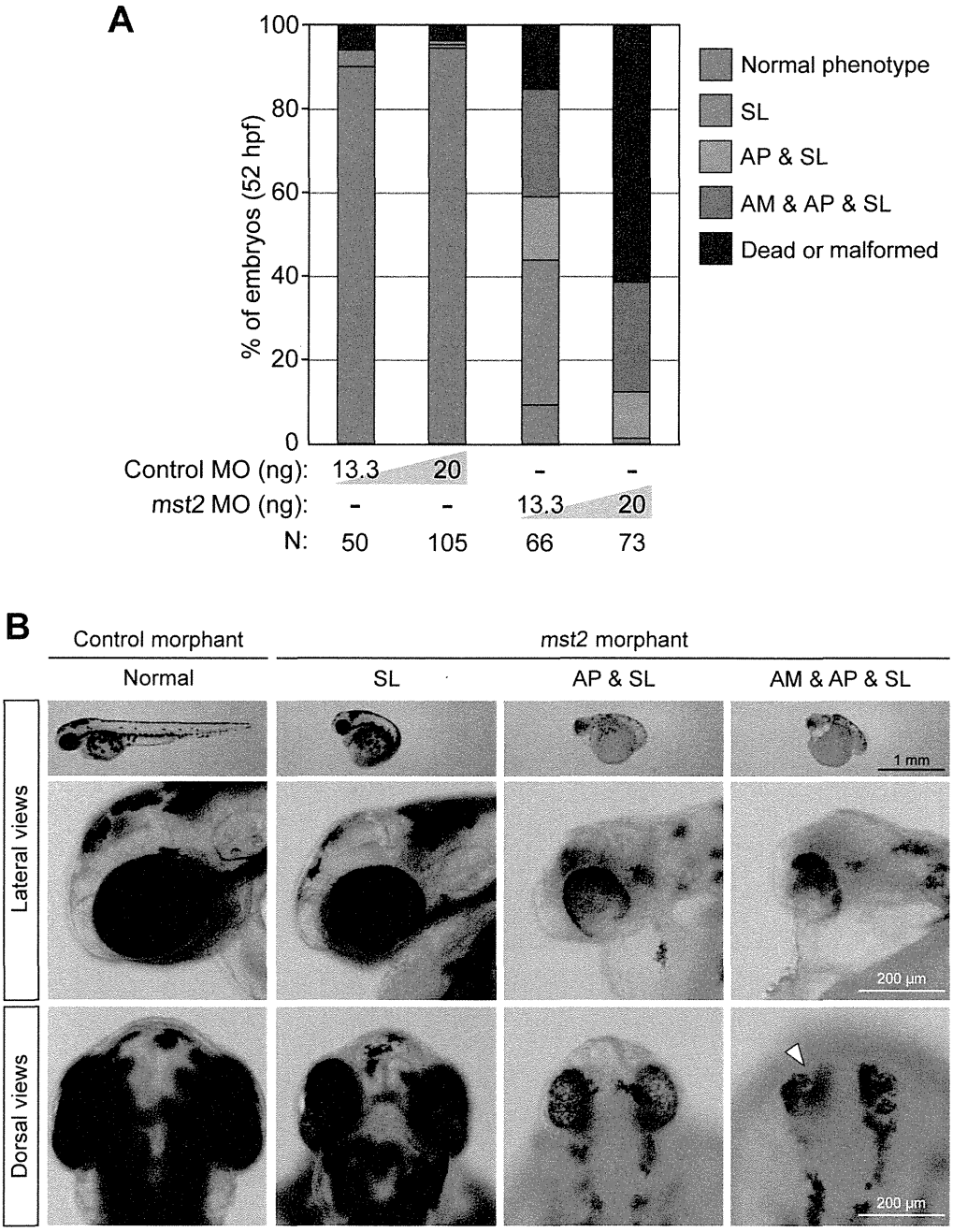

Figure 1. Mst2 is essential for early zebrafish embryogenesis. (A) Early developmental abnormalities of *mst2* morphants. Control or *mst2* morpholino (MO) at the indicated dose was injected into zebrafish embryos and phenotypes were analyzed at 52 hpf. Embryos were classified into five color categories on the basis of their phenotypes: blue, normal embryos; green, short body length (SL); orange, abnormal eye pigmentation (AP) accompanied by SL; red, abnormal eye morphology (AM) plus AP plus SL; and brown, dead or malformed embryos. Results are presented as the percentage of the total number of embryos examined (N). (B) Representative control and *mst2* morphants at 52 hpf. Embryos were injected with control MO (13.3 ng) or *mst2* MO (13.3 ng). Top panels, lateral views of whole embryos. Middle panels, higher magnification images of the head regions of the embryos in the top panels. Bottom panels, dorsal views of the head regions of the embryos in the top panels. (The head is at the top of each panel.) White arrowhead, representative area of AM.
doi:10.1371/journal.pone.0097365.g001

control of the zebrafish heat shock-inducible promoter *hsp70* [*hsp70-EGFP-yap (5SA)*] [22], and induced *yap (5SA)* expression only after 21 hpf (Fig. 4A). Whereas injection alone of *hsp70-EGFP-yap (5SA)* induced no phenotypic alterations, heat shock applied at 21 hpf after injection of *hsp70-EGFP-yap (5SA)* gave rise to abnormal retinal phenotypes (AM and/or AP) (Fig. 4B and 4C). It is noteworthy that, although many embryos also exhibited the SL phenotype (AP+SL, 48%; AM+AP+SL, 9%; N = 23), a sizable proportion showed only an abnormal retinal phenotype (AP, 17%; N = 23). These results support our hypothesis that Yap activity has a direct impact on retinal development.

To achieve retina-specific expression of Yap, we generated a construct containing the upstream region (including the promoter) of the medaka *rx3* gene [*rx-EGFP-yap (5SA)*]. Injection of this

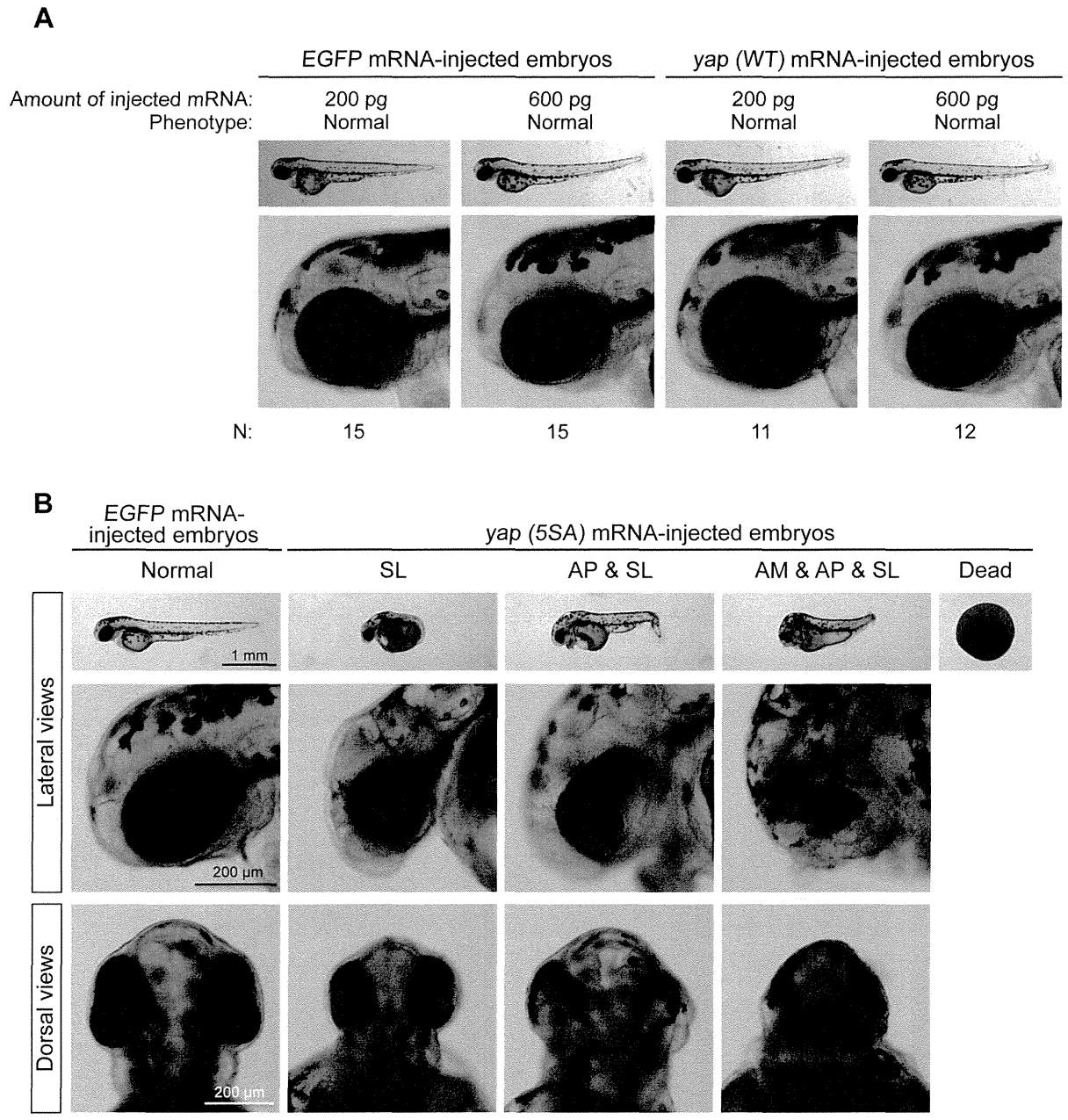

Figure 2. Forced expression of mRNA encoding constitutively active *yap* alters early zebrafish embryogenesis. (A) Representative images of *EGFP* mRNA-injected (control) or *yap (WT)* mRNA-injected zebrafish embryos at 52–54 hpf. Top panels, lateral views of whole embryos. Bottom panels, higher magnification images of the head regions of the embryos in the top panels. N, total number of embryos examined. Embryos injected with either *yap (WT)* mRNA or *EGFP* mRNA had normal phenotypes. (B) Representative images of *EGFP* mRNA-injected (control) or *yap (5SA)* mRNA-injected zebrafish embryos at 48 hpf. Embryos injected with *Yap (5SA)* mRNA (10 pg) showed the same spectrum of abnormal phenotypes as *mst2* morphants. Data are presented as for Fig. 1B.
doi:10.1371/journal.pone.0097365.g002

plasmid into zebrafish embryos resulted in expression of *yap (5SA)* preferentially in the retina (Fig. 5A). Expression of *rx-EGFP-yap (5SA)* gave rise to abnormal eye phenotypes (AM and/or AP) in about 60% of injected embryos (AP, 29%; AM+AP, 31%; N = 45), with no detectable effect on body axis (Fig. 5B and 5C). Conversely, expression of *yap (5SA)* variants mutated in both WW domains [*rx-EGFP-yap (5SA/WW1*, 2*)*] prevented the appearance of abnormal eye phenotypes. These data demonstrate that the two WW domains of Yap mediate activity that directly affects zebrafish retinogenesis.

Retinal Photoreceptor Genes are Downregulated in *yap (5SA)*-expressing Embryos

To conduct a comprehensive survey of transcriptional targets activated downstream of Hippo-Yap signaling during early zebrafish development, we employed a microarray approach and compared genome-wide transcriptomes between *yap (WT)*- and *yap (5SA)*-expressing embryos at three developmental stages (42, 48 and 54 hpf). Gene ontology (GO) analysis revealed that the top two GO categories for genes showing a >4.0-fold decrease in expression in *yap (5SA)*-expressing embryos at each stage were

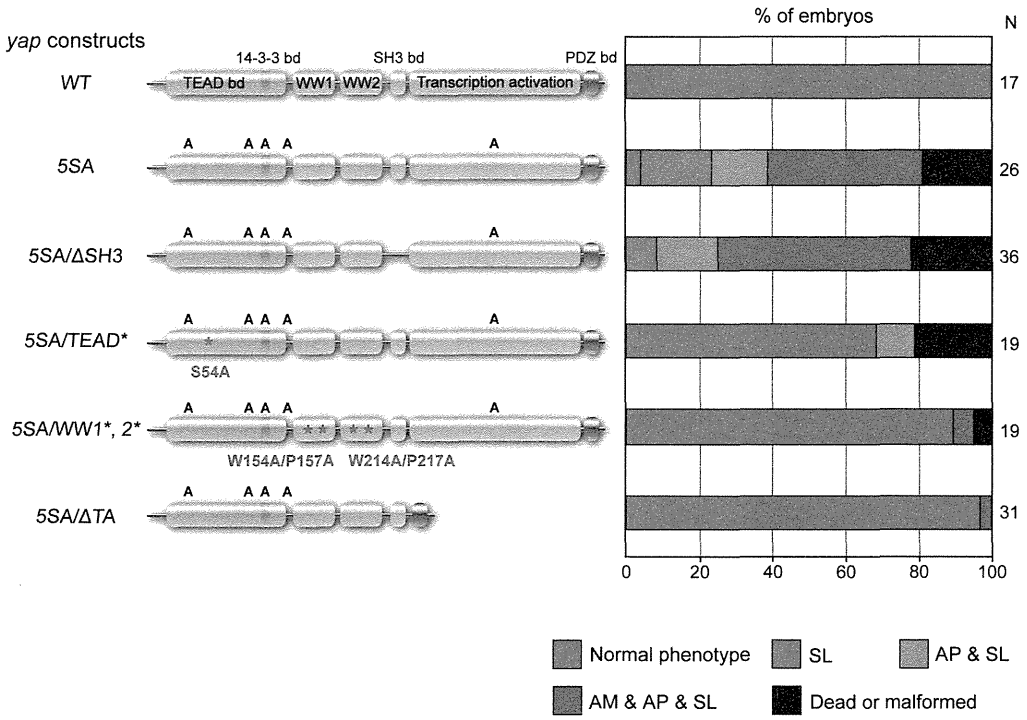

Figure 3. The TEAD-binding, WW and transcription activation domains of Yap contribute to early zebrafish development. Left panel, schematic illustration of constructs of Yap (WT), Yap (5SA), and the indicated variants with deletion (Δ) or mutation (*) of the indicated domains. Specific amino acid alterations are indicated. A, Lats phosphorylation site replaced by an alanine. *In vitro*-synthesized mRNAs (10 pg) derived from these constructs were injected into zebrafish embryos and phenotypes were quantified as shown in the right panel. Color classification is as for Fig. 1A. Results are presented as the percentage of the total number of embryos examined (N).
doi:10.1371/journal.pone.0097365.g003

"phototransduction" and "detection of light stimulus" (Fig. 6A). Strikingly, the retinal photoreceptor gene *rhodopsin* was the gene most downregulated in *yap (5SA)*-expressing embryos compared to *yap (WT)*-expressing embryos (Fig. 6B). This remarkable decrease was 17.0-fold at 42 hpf, an enormous 1,974-fold at 48 hpf, and 449-fold at 54 hpf. Moreover, we found that expression levels of genes encoding photoreceptor TFs such as *crx*, *nr2e3* and *otx5*, which are required for *rhodopsin* transcription [23–25], were greatly reduced in *yap (5SA)*-injected embryos (decreased by 157-, 58.8-, and 29.1-fold, respectively, at 48 hpf) (Fig. 6B). These results indicate that the expression of *yap (5SA)* mRNA affects the transcription of retinal photoreceptor genes.

To confirm Yap's influence on retinal gene expression, we carried out a detailed RT-PCR analysis of mRNA levels in *yap (5SA)*-injected embryos and *mst2* morphants. We found that mRNA levels of *otx2*, *otx5*, *crx* and *rhodopsin* were all dramatically downregulated in *yap (5SA)*-injected embryos at 48 hpf compared to *yap (WT)*-injected embryos (Fig. 6C). *Mst2* morphants also displayed decreased mRNA expression of the *otx2*, *crx*, and *rhodopsin* genes (Fig. S3A and S3B). Lastly, because Rx is known to be an upstream transactivator that regulates *otx2* and *rhodopsin* expression in mice and *Xenopus* [9,26], we examined whether expression of the *rx1* and *rx2* genes was reduced in *yap (5SA)*-expressing embryos. Interestingly, levels of *rx1* and *rx2* mRNAs in *yap (5SA)*-injected embryos were comparable to those in *yap (WT)*-injected embryos (Fig. 6C). These results suggest that Yap activity affects zebrafish retinogenesis via transcriptional regulation of photoreceptor genes acting downstream of the *rx* genes.

The Photoreceptor Cell Differentiation Factor Rx1 is a Novel Interacting Partner of Yap

The above microarray and RT-PCR analyses suggested that activated Yap might suppress photoreceptor cell differentiation through interactions with TF(s) acting upstream of *otx*, *crx* and *rhodopsin*. We investigated Rx1 as a candidate TF in this context because zebrafish Rx1 reportedly plays a prominent role in the regulation of retinal photoreceptor differentiation [27]. Intriguingly, we found that zebrafish Rx1 contains an evolutionarily conserved PPXY motif that interacts with Yap's WW domains (Fig. 7A), whereas none of the other three photoreceptor TFs examined (Otx2, Otx5 and Crx) contains a PPXY motif. This observation prompted us to use co-immunoprecipitation analysis to investigate whether Yap and Rx1 could physically interact with each other in cells. Myc-Rx1 was co-expressed with FLAG-Yap (5SA), FLAG-Yap (5SA/WW1*, 2*), or FLAG-Yap (5SA/TEAD*) in HEK293T cells, and cell lysates were subjected to immunoprecipitation with anti-FLAG antibody. We observed that Myc-Rx1 successfully co-immunoprecipitated with either FLAG-Yap (5SA) or FLAG-Yap (5SA/TEAD*) but not with FLAG-Yap (5SA/WW1*, 2*) (Fig. 7B). These results demonstrate that Rx1 can indeed interact with Yap, and that this interaction is mediated by Yap's two WW domains. We also co-expressed FLAG-Yap (5SA) with Myc-Rx1 missing its PPXY motif [Myc-Rx1 (ΔPPXY)] in HEK293T cells and subjected cell lysates to immunoprecipitation with anti-FLAG antibody. Myc-Rx1 (ΔPPXY) did not co-immunoprecipitate with FLAG-Yap (5SA) (Fig. 7C), indicating that the PPXY motif of Rx1 is essential for its interaction with Yap. These data identify the photoreceptor cell differentiation factor Rx1 as a novel interacting partner of Yap, and suggest that

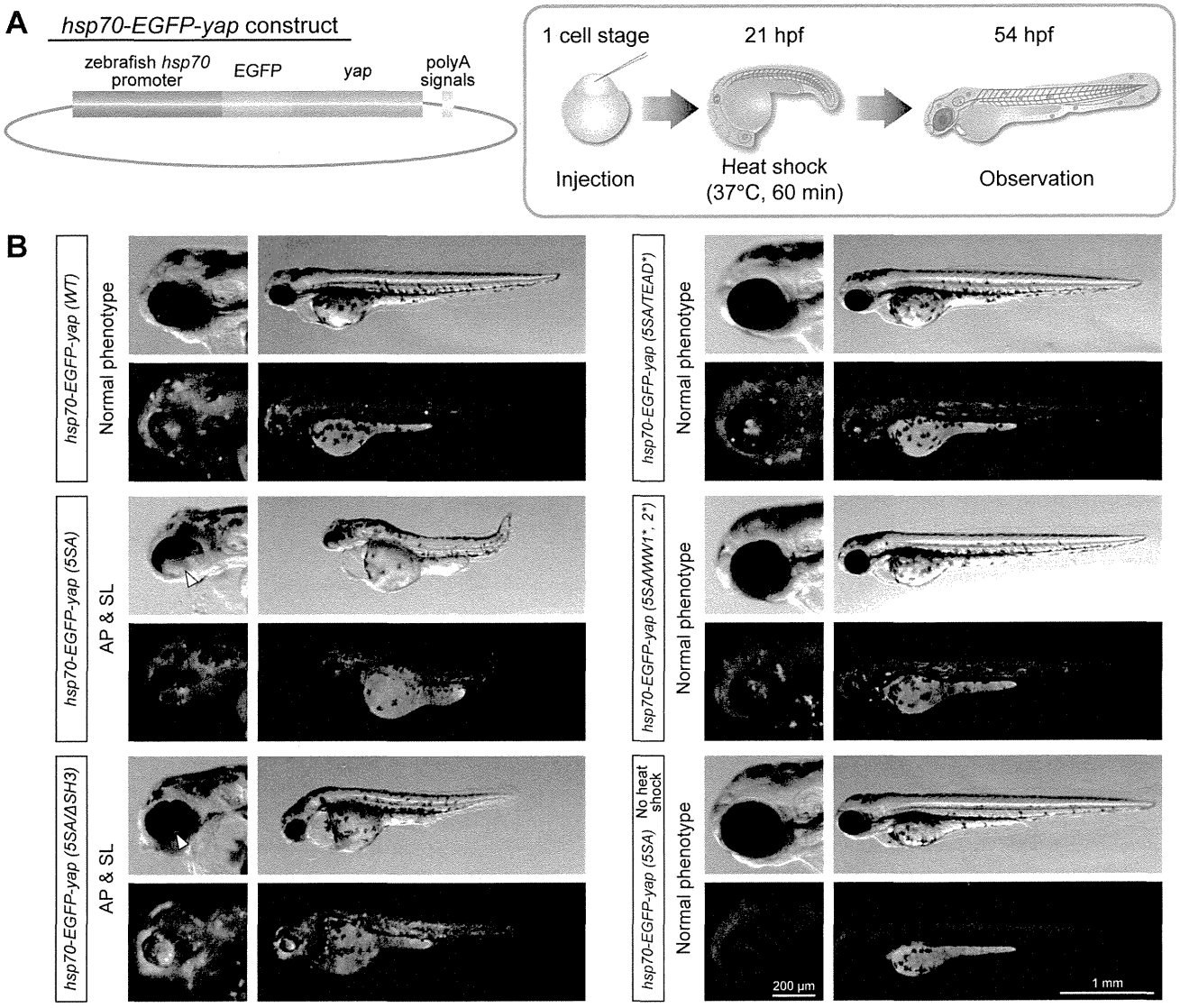
A
hsp70-EGFP-yap construct
zebrafish hsp70 promoter
EGFP
yap
polyA signals
1 cell stage
21 hpf
54 hpf
Injection
Heat shock (37°C, 60 min)
Observation
B
hsp70-EGFP-yap (WT)
Normal phenotype
hsp70-EGFP-yap (5SA)
AP & SL
hsp70-EGFP-yap (5SA/ΔSH3)
AP & SL
hsp70-EGFP-yap (5SA/TEAD*)
Normal phenotype
hsp70-EGFP-yap (5SA/WW1*, 2*)
Normal phenotype
hsp70-EGFP-yap (5SA) No heat shock
Normal phenotype
200 µm
1 mm
C
hsp70-EGFP-yap constructs
14-3-3 bd
SH3 bd
PDZ bd
WT
TEAD bd
WW1
WW2
Transcription activation
5SA
5SA/ ΔSH3
5SA/ TEAD*
S54A
5SA/ WW1*, 2*
W154A/P157A
W214A/P217A
% of embryos (54 hpf)
N
4
23
16
12
12
0
20
40
60
80
100
Normal phenotype
SL
AP
AP & SL
AM & AP & SL

Figure 4. Yap is directly involved in zebrafish retinogenesis. (A) Schematic illustration of the base *hsp70-EGFP-yap* construct (left panel) and the procedure for the heat shock experiment (right panel). Zebrafish embryos at the one-cell stage were injected with plasmid DNA containing the heat shock promoter constructs indicated in (B). At 21 hpf, injected embryos were immersed in a 37°C water bath for 1 h to apply heat shock and thus induce expression of EGFP-fused Yap. At 54 hpf, EGFP-expressing embryos were isolated and classified on the basis of their phenotypic features. (B) Representative images of the embryos in (A) that were injected with heat shock promoter constructs as indicated on the left side of panels. For each column, top right panels show lateral views of whole embryos, top left panels show higher magnification images of the head regions of the embryos, and bottom panels are fluorescent images of the corresponding top panels. White arrowheads, areas of AP. (C) Quantification of phenotypes of the embryos injected with heat shock promoter constructs in (A, B) as analyzed at 54 hpf. Color classification is as for Fig. 1A except that the phenotype of AP alone is indicated by striped orange shading. Results are presented as the percentage of the total number of embryos examined (N).
doi:10.1371/journal.pone.0097365.g004

Yap may be crucial for coordinating the timing of the terminal differentiation of photoreceptor neurons by suppressing the transcription of the *otx*, *crx* and *rhodopsin* genes.

Discussion

In this study, we examined the role of Hippo-Yap signaling during zebrafish retinogenesis by carrying out an *in vivo* analysis. We demonstrated that knockdown of Mst2 or forced expression of *yap (5SA)* not only disrupts normal embryogenesis as a whole but has specific detrimental effects on retinal pigmentation, eye morphology, and the expression of retinal photoreceptor genes. With respect to embryogenesis, the SL phenotype we observed in our *yap (5SA)* mRNA-injected embryos at 18–21 hpf (Fig. S2C) is similar to that of morphants created in a previous study by knockdown of the zebrafish *yap* gene [17,28]. These latter morphants exhibited a shortened body axis and elevated expression of the somite marker *myoD* during somitogenesis. Our findings thus provide additional evidence that strict control of the activity and localization of Yap is essential for normal somitogenesis during the earliest stages of embryogenesis. Moreover, our data show that Hippo-Yap signaling acts at a later developmental stage as a crucial switch governing retinogenesis.

A key result of our paper is that Yap and the retina-specific TF Rx1 physically interact with each other through Yap's WW domains and Rx1's PPXY motif. Fig. S4 illustrates our proposed model for the bifunctional involvement of Hippo-Yap signaling in determining RPC proliferation versus photoreceptor cell differentiation. When the Hippo pathway is inactive, Yap is activated and associates with TEAD to help drive expression of proliferation-related genes. Simultaneously, activated Yap binds to Rx1 and attenuates its transactivation of photoreceptor genes. The result is the expansion of RPCs and the suppression of photoreceptor cell differentiation. However, when the Hippo pathway is activated by a developmental cue, Yap activation is blocked and the expression of photoreceptor genes is upregulated, promoting the differentiation of mature photoreceptor cells. Thus, in this model, Hippo-Yap signaling is the key molecular mechanism governing the decision of an RPC to self-renew or differentiate.

In *Drosophila*, Hippo is the homolog of mammalian Mst2. In the *Drosophila* eye, Hippo is involved in post-mitotic fate-determining events such as photoreceptor subtype specification [29]. It is conceivable that the primary role of Mst2 in the developing eye is evolutionarily conserved among vertebrate species. In our study of MO-mediated knockdown of zebrafish *mst2*, we showed that this gene is essential for retinal photoreceptor differentiation (Fig. 1A, 1B and S3). In *Xenopus*, Nejigane *et al.* [2013] carried out a loss-of-function analysis of *mst1/2* and found that *mst2* morphants displayed morphogenetic defects, including abnormally small eyes [30]. However, it has been difficult to determine the separate physiological functions of the mammalian *Mst1* and *Mst2* genes during retinal development due to their overlapping tissue expression and functional redundancy. For example, both the *Mst1* KO and *Mst2* KO single null mutant strains are viable and develop normally, suggesting a substantial functional overlap between these two paralogs [31]. Further functional analysis of *Mst1/2* genes in other vertebrates should help to reveal more about the possible evolutionary diversion of Mst1 and Mst2.

Previous studies have implicated Hippo signaling in ocular development [11,16,17,30]. For example, Zhang *et al.* observed that forced expression of Yap in mouse retina prevented proneural bHLH proteins from inducing cell cycle exit, whereas inhibition of Yap decreased RPC proliferation and increased retinal cell differentiation [11]. However, few studies have focused on the molecular mechanism(s) by which Hippo-Yap signaling regulates the differentiation of specific neuronal subtypes such as photoreceptor cells. In our study, we demonstrated that at least three photoreceptor TFs (Otx2, Otx5 and Crx) are activated downstream of Hippo signaling (Fig. 6C and S3). In addition, we discovered that Rx1 is a novel interacting partner of Yap (Fig. 7B), a finding that supplies a missing piece of the puzzle concerning the molecular basis of Hippo-Yap-mediated effects on photoreceptor cell differentiation. In mouse studies, Rx is essential for *otx2* transactivation in the embryonic retina [9]. In *Xenopus* retina, Rx reportedly plays a role in the transcriptional regulation of other retinal photoreceptor genes, such as *rhodopsin* and *red cone opsin* [26]. In zebrafish, Rx1 is required for photoreceptor differentiation [27]. These previous results, together with our present study, support the idea that the timing of activation of both the Rx1-*otx/crx* and Rx1-*rhodopsin* transcriptional cascades is regulated by the Hippo-Yap pathway during zebrafish photoreceptor development.

Our mutational analysis of the Yap (5SA) protein demonstrated that Yap's TEAD-binding, WW, and transcription activation domains all play a pivotal role in the regulation of retinogenesis (Fig. 3). TEAD family members have previously been shown to be critical partners of Yap in regulating neural progenitor cells. For example, Yap functions through TEAD family members to control the proliferation of progenitors in the chicken spinal cord [32]. In the *Xenopus* neural plate, Yap and TEAD1 cooperate to expand neural progenitors and directly regulate *pax3* expression [21]. Our study therefore provides more evidence that the precise regulation of Yap-TEAD interaction is important for maintaining normal neurogenesis. In addition to TEAD family members, PPXY motif-containing TFs, such as ErbB4, p73 and RUNX2, have been shown to interact with Yap via its WW domains [33–35]. For instance, Yap suppresses RUNX2-dependent transcriptional activation of the *osteocalcin* gene promoter [36]. Our study identifies zebrafish Rx1 as a novel photoreceptor differentiation factor, and shows that Rx1's PPXY motif interacts with the WW domains of Yap. This result is consistent with previous observations that many protein interactions associated with Hippo-Yap signaling rely on the binding of a protein's PPXY motif to Yap's WW domains [37–39]. We postulate that Yap functions as a bifunctional transcriptional cofactor by using its TEAD-binding or WW domains; i.e., Yap co-activates the proliferation of RPCs induced by TEAD family members, but also co-represses retinal photoreceptor

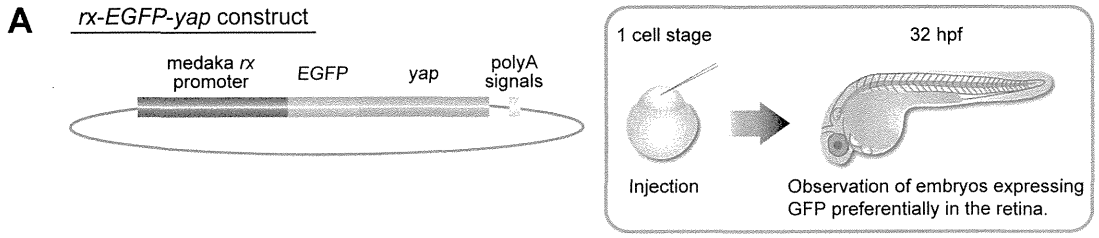
A
rx-EGFP-yap construct
medaka rx promoter
EGFP
yap
polyA signals
1 cell stage
32 hpf
Injection
Observation of embryos expressing GFP preferentially in the retina.

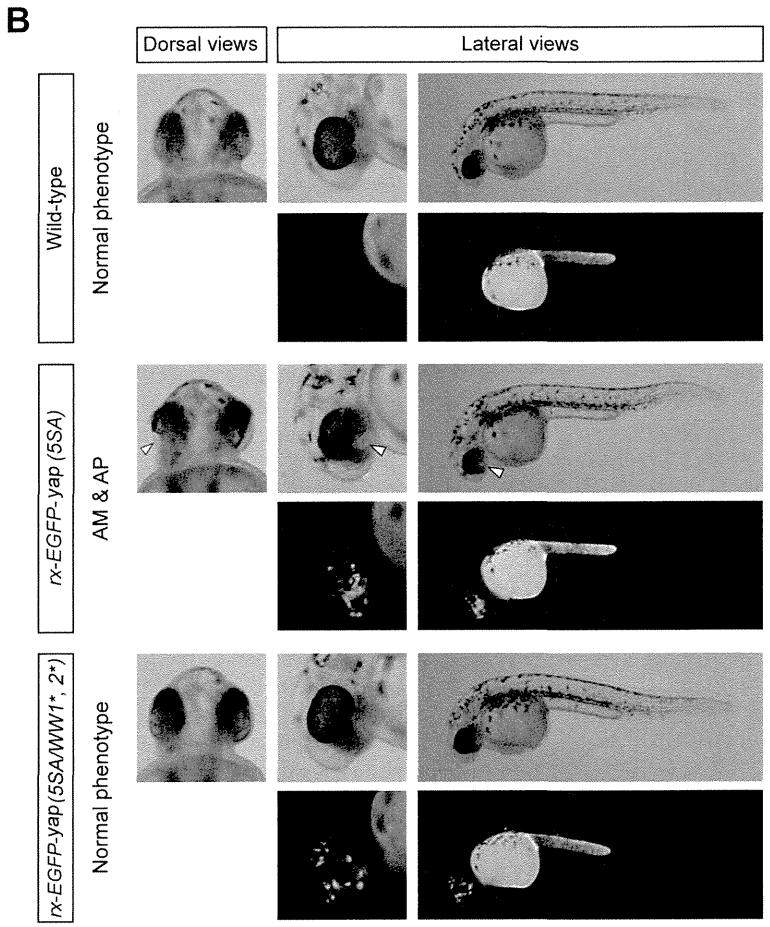
B
Dorsal views
Lateral views
Wild-type
Normal phenotype
rx-EGFP-yap (5SA)
AM & AP
rx-EGFP-yap (5SA/WW1*, 2*)
Normal phenotype

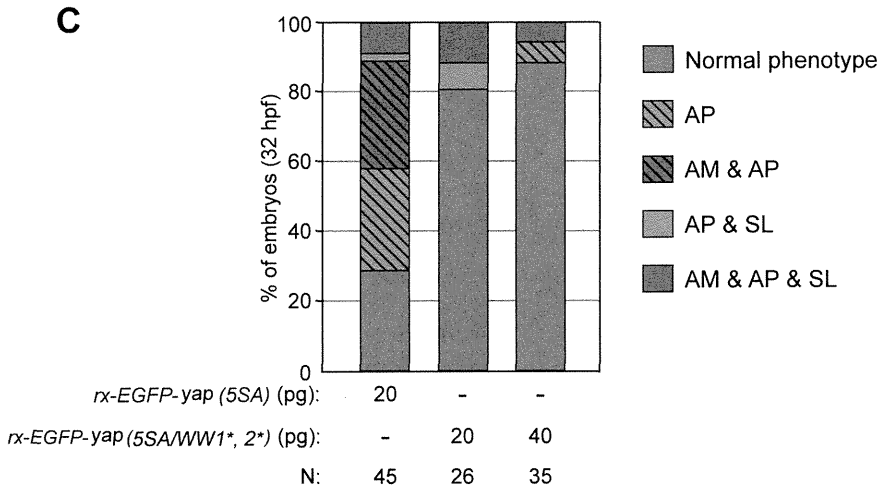
C
100
80
60
40
20
0
% of embryos (32 hpf)
Normal phenotype
AP
AM & AP
AP & SL
AM & AP & SL
rx-EGFP-yap (5SA) (pg): 20 - -
rx-EGFP-yap (5SA/WW1*, 2*) (pg): - 20 40
N: 45 26 35

Figure 5. Retina-specific expression of *yap (5SA)* induces retinogenesis defects without affecting body axis formation. (A) Schematic illustration of the base *rx-EGFP-yap* construct (left panel) and the procedure for the experiment (right panel). Zebrafish embryos at the one-cell stage were injected with plasmid DNA containing the *rx* promoter constructs indicated in (B). (B) Representative dorsal and lateral views of the embryos in (A) that were injected with *rx* promoter constructs as indicated on the left side of panels. Data are presented as for Fig. 4B. White arrowheads, areas of AM plus AP. (C) Quantification of phenotypes of the embryos injected with *rx* promoter constructs in (A, B) as analyzed at 32 hpf. Color classification is as for Fig. 4C except that the phenotype of AM plus AP is indicated by striped red shading. Results are presented as the percentage of the total number of embryos examined (N). Note that expression of *yap (5SA)* variants mutated in both the WW1 and WW2 domains prevented the appearance of abnormal eye phenotypes.
doi:10.1371/journal.pone.0097365.g005

differentiation through interaction of its WW domains with Rx1 (Fig. S4).

It is worth noting that the zebrafish genome contains additional PPXY motif-containing retinal TFs, including ROR members and Nrl (Fig. S5B and S5C); these proteins could also be potential Yap targets. In particular, zebrafish RORα and RORβ possess a PPXY motif that is highly conserved among vertebrate species (Fig. S5B). Furthermore, RORα and RORβ are known to be crucial for photoreceptor cell differentiation because they directly regulate multiple photoreceptor genes [40–42]. Further analyses of TFs expressed in vertebrate photoreceptor tissues should help to evaluate the general role of Yap in photoreceptor cell differentiation.

Yap and its paralogous coactivator TAZ are central nuclear effectors of Hippo signaling and play critical roles in early development [43]. In most vertebrates, Yap occurs both in the Yap1-1 isoform, which has a single WW domain, and in the Yap1-2 isoform, which has tandem WW domains [44]. In contrast, vertebrate TAZ occurs almost exclusively in an isoform with a single WW domain [45]. Recently, a second TAZ isoform was identified in medaka that possesses tandem WW domains like the Yap1-2 isoform [45]. In this study, the affinity between TAZ and PPXY-containing ligands was enhanced by the presence of the additional WW domain, potentially affecting partner protein selection. However, it remains to be determined whether the second TAZ isoform shares binding partners and functional redundancy with the Yap1-2 isoform during early fish development.

Our studies have demonstrated that active Yap can repress retinal photoreceptor cell differentiation, at least in part, by directly blocking the Rx transcriptional machinery. However, the upstream factors that control the timing of Hippo-Yap activation remain unknown. It is possible that the apicobasal polarity protein Crumbs (CRB) is a candidate upstream sensor regulating Yap activity during retinogenesis. Pellissier *et al.* have recently reported that the loss of both CRB1 and CRB2 during early retinogenesis in mice prevents the development of a separate photoreceptor layer and leads to a loss of retinal function that is reminiscent of the abnormalities of humans with Leber Congenital Amaurosis [46]. Pellissier *et al.* also showed that the transcription of *connective tissue growth factor*, a Yap-regulated gene, was reduced in CRB1/CRB2 double KO mice [46], suggesting a critical role for CRB in regulating Yap activity and RPC proliferation during vertebrate retinogenesis. Other cell-extrinsic signals, such as mechanical forces, GPCR ligands, cell density, and serum concentration, have been shown to regulate the Hippo pathway during tissue-specific stem cell differentiation [47]. Understanding exactly how such a variety of microenvironmental signals might coordinate Hippo pathway signaling during RPC/photoreceptor cell fate determination awaits future study.

Materials and Methods

Statement on the Ethical Treatment of Animals

This study was carried out in strict accordance with the recommendations in the ethical guidelines of Tokyo Medical and Dental University. All experimental protocols in this study were approved by the Animal Welfare Committee of Tokyo Medical and Dental University (Permit Number: 2010-212C). All experiments were performed in a manner that minimized pain and discomfort.

Zebrafish Maintenance and Staging

The TL wild type (WT) strain was maintained essentially as described in "The Zebrafish Book" [48]. Embryos were produced by natural matings and staged by standard morphological criteria or by hours or days post-fertilization (hpf or dpf), as described [49].

Phylogenetic Tree

Amino acid sequences of Mst1 and Mst2 of various species were obtained from the Ensembl database. The Ensembl ID numbers of the sequences used were as follows: human MST1 (ENSP00000361892), mouse MST1 (ENSMUSP00000018353), *Xenopus* Mst1 (ENSXETP00000049383), medaka Mst1 (ENSORLP00000024937), pufferfish Mst1 (ENSTNIP00000007894), stickleback Mst1 (ENSGACP00000000023), human MST2 (ENSP00000390500), mouse MST2 (ENSMUSP00000018476), *Xenopus* Mst2 (ENSXETP00000038688), zebrafish Mst2 (ENSDARP00000015367), medaka Mst2 (ENSORLP00000023002), pufferfish Mst2 (ENSTNIP00000012004), stickleback Mst2 (ENSGACP00000004790) and *Drosophila* Hippo (FBpp0085688). A Genescan prediction from the Ensembl database was used to obtain the complete medaka Mst2 sequence. These amino acid sequences were aligned with each other and any positions containing gaps were eliminated. The phylogenetic tree was constructed using the neighbor-joining method and ClustalX software [50]. The reliability of the tree was estimated using the bootstrap method and 10,000 replications.

Antisense Morpholino (MO) against *mst2*

The *mst2* MO (5′-ATGGG CTGTT AAAAC ACAAT GAGGA-3′) was designed to target the splice acceptor site of exon 4 of the zebrafish *mst2* gene (ENSDARG00000011312) and was synthesized by GeneTools, LLC (Philomath, OR). For knockdown, *mst2* MO solution (13.3 or 20 ng) was injected into the yolks of one-cell to four-cell stage zebrafish embryos immediately beneath the cell body. The standard negative control MO (5′-CCTCT TACCT CAGTT ACAAT TTATA-3′) was injected into a control cohort of zebrafish embryos in a similar fashion. Reduction in *mst2* mRNA was confirmed by RT-PCR analysis using the oligonucleotide primer pair 5′-AGCCA TTCAC AAGGA ATCAG G-3′ and 5′-GGTAA GTTGT CCAGC TACTC C-3′.

A

log_2 [Yap (5SA)/ Yap (WT)] < -2.0		
Rank	**Gene Ontology**	**Score (p value)**
1	Phototransduction (GO:0007602)	2.97E-59
2	Detection of light stimulus (GO:0009583)	2.98E-57
3	Detection of abiotic stimulus (GO:0009582)	5.10E-56
4	Detection of external stimulus (GO:0009581)	2.39E-49
5	System process (GO:0003008)	3.91E-44

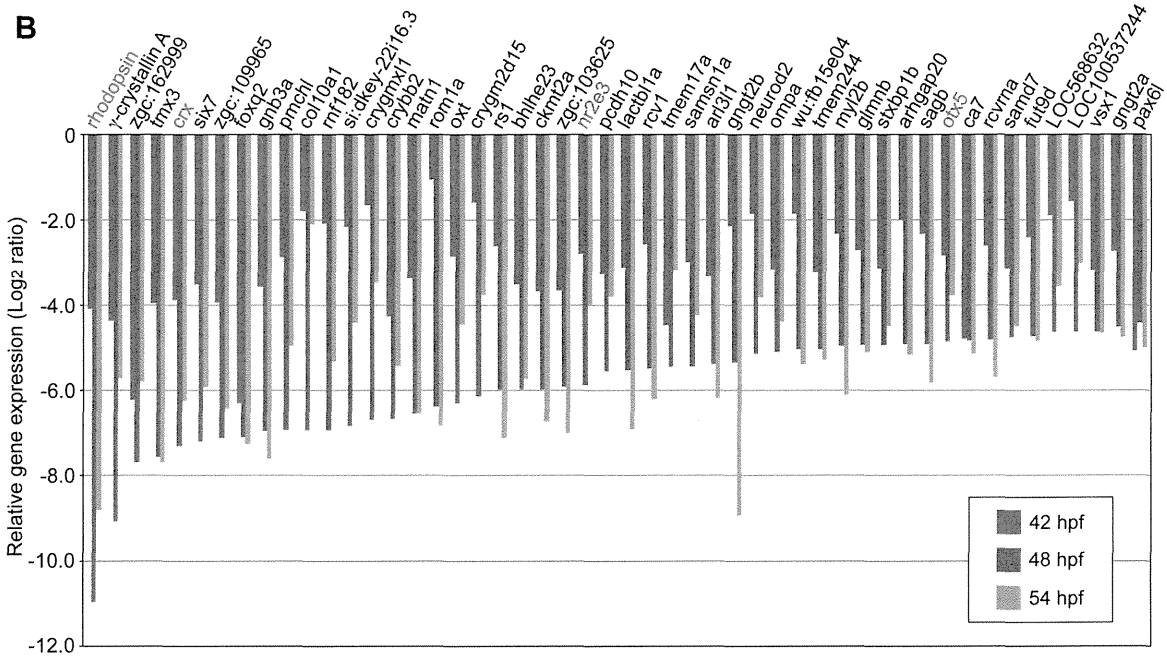

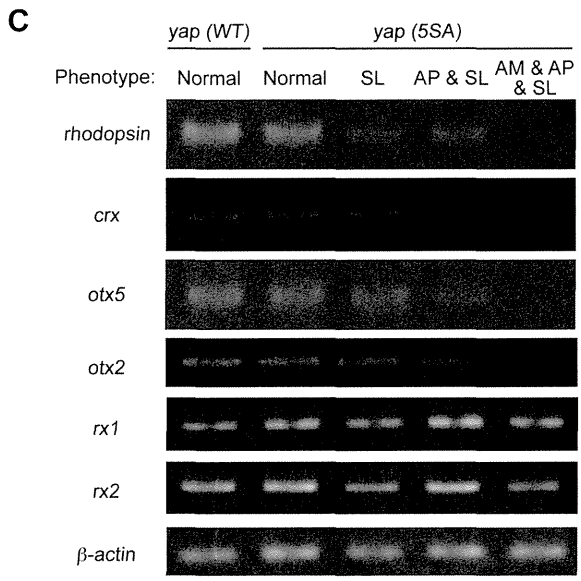

Figure 6. ***Yap (5SA)*** **mRNA-injected embryos exhibit dramatic downregulation of retinal photoreceptor genes.** (A) The top five GO categories for genes downregulated by over 4.0-fold in *yap (5SA)*-expressing embryos at 48 hpf as determined by microarray analysis. (B) A summary of microarray results for the top 50 downregulated genes in the *yap (5SA)*-expressing embryos in (A) compared with *yap (WT)*-expressing embryos at 42, 48 and 54 hpf. The expression levels of genes in the *yap (5SA)*-injected embryos are shown as Log_2 (fold change) values relative to *yap (WT)*-injected embryos. The order of the genes is based on expression levels detected at 48 hpf. Red lettering indicates retinal photoreceptor genes whose expression was severely decreased in *yap (5SA)*-injected embryos. (C) RT-PCR analysis of mRNA expression of the indicated retinal genes in zebrafish embryos injected with *yap (WT)* or *yap (5SA)* mRNA and examined at 48 hpf. β-actin, loading control. *Yap (5SA)*-expressing embryos are grouped by abnormal phenotype, as indicated. Results are representative of two independent experiments.
doi:10.1371/journal.pone.0097365.g006